A NOVEL MULTISCALE MODEL FOR MICRO-STRUCTURED ELECTROMAGNETIC MEDIA

P.J. BLANCO, F.A. PINHEIRO, AND A.A. NOVOTNY

Abstract. We present a novel multiscale formalism to characterize complex phenomena in electromagnetic media featuring micro-structures. In contrast to the conventional homogenisation approaches, the proposed model is based on the variational framework given by the Method of Multiscale Virtual Power applied to Maxwell's equations, which ensures energetic consistency between the macro- and micro-scales. From a set of well-defined minimal assumptions on the primal variables, the electromagnetic field and its curl, the formulation yields not only the micro-cell problem to be solved but also the homogenisation formulae of the dual entities, as well as the homogenisation of tangent operators that characterize, for instance, the effective electric permittivity and magnetic permeability. The proposed multiscale model is not restricted to periodic media, although it accounts for the periodicity assumption as a specific case. We apply the method in different cases of interest that range from low-frequency to high-frequency regimes to demonstrate the predictive and descriptive capabilities of the model in terms of effective electromagnetic properties.

1. Introduction

In the past two decades, research in the field of electromagnetic metamaterials has been attracting increasing interest, opening unprecedented avenues for both basic research and applications. Investigation of micro-structured materials, specifically engineered to feature desired electromagnetic properties permeates many research domains such as physics, chemistry, material science, and engineering. These technological innovations encompass the whole electromagnetic spectrum, from microwave to optical applications.

Applications of metamaterials usually aim at achieving unusual electromagnetic properties and functionalities such as optimised absorbers [43, 39], negative index and chiral metamaterials [35, 26], tunable metasurfaces [1], and all-dielectric metamaterials for nanophotonic applications [24]. Among the many technological applications, one can mention the design of isolators and circulators through asymmetric transmission properties [32], and the use of plasmonic metamaterials for optical sensing [40, 41].

Traditionally, in the domain of metamaterials technological development and experimental activities are unceasingly supplemented by numerical simulations [36, 16]. Moreover, modelling and simulation also offer the possibility of conceiving novel, designed materials with desired properties, by engineering-reversing the micro-scale structure to target a desired macro-scale behavior. It is important to emphasize that in this contribution we refer to micro- and macro-scale as synonyms for small-scale and large-scale phenomena. The numerical modelling of constitutive parameters in the presence of these unusual, extreme scenarios is typically challenging.

In such a context, research in the field of scientific computing and applied mathematics has approached the problem of building multiscale theories for Maxwell's equations. The

Date: October 2, 2024.

Key words and phrases. Maxwell's equations, variational formulation, multiscale modelling, homogenisation, metamaterials, effective permittivity.

purpose of these theories is to upscale micro-scale wave phenomena and to properly characterize the emergent electromagnetic properties of such micro-structured materials. Such an approach to the constitutive modelling of electromagnetic media is promising since it allows for a physically consistent characterisation, as it is based on the fundamental laws of electromagnetism working on top of a certain arrangement of constituents within a so-called micro-cell.

The development of multiscale models for electromagnetic phenomena presents a myriad of approaches. Indeed, one of the landmark contributions has been put forward in [44] which presents a two-scale convergence analysis to study the homogenisation of Maxwell's equations, under the hypothesis of long wavelengths compared to the characteristic length of the micro-cell. A similar approach was used to study material tilings of quasi-crystals with specific symmetry properties [13]. Using asymptotic analysis, in [5] the authors studied the homogenisation of Maxwell's equations for low and high-frequency regimes. Also using two-scale convergence analysis, in [14] the authors derive the effective properties for a complex micro-cell arrangement in order to characterize materials with negative permeability due to resonance phenomena. As alternative multiscale modelling, it can be mentioned the use of the periodic unfolding method in [7] to obtain effective electromagnetic properties in the low-frequency regime, and the use of an optimisation approach [38], to characterize the effective properties based on pre-defined quantities of interest and for simple micro-cell configurations.

Multiscale modelling aims at bringing into the effective properties at the macro-scale, high-order phenomena retrieved from the micro-cell problem. In this sense, Ref. [17] proposed, for the low-frequency regime, a high-order model where the magnetic and electric fields are functions of the magnetic induction and its spatial gradients, respectively, and of the displacement field and its spatial gradients. This is in the spirit of high-order continua pursued in [22], and more recently in [21].

Most of the previous studies employed the two-scale convergence framework of analysis for multiscale modelling developed by [3, 29]. In turn, an alternative approach consists of using the so-called Bloch wave expansion of the physical fields to characterize the spectral behavior of the material [4]. One of the advantages is that this spectral approach allows for going beyond the low-frequency regime, as it has been done in [27]. However, the characterisation of effective properties such as electric permittivity and magnetic permeability can only be performed under additional hypotheses regarding the frequency. Bloch wave expansions were also used in [6] to propose a micro-cell problem-free strategy to characterize the effective properties. Similarly, in [18] Bloch expansion is used to characterize the spectral behavior of materials and also to obtain effective properties for very specific topological arrangements of the phases in the micro-cell. Bloch wave representation was also employed in [2] to treat a composite made of a metamaterial with frequency-dependent permittivity that exhibits resonant behavior, and this strategy is used to tune frequency-dependent effective properties, leading to double negative metamaterials in certain frequency intervals. Using a spectral approach, in [34] it is derived a general numerical approach to compute effective properties in arbitrary non-magnetic metamaterials, where the effective electric permittivity is computed by solving an integro-differential equation. Similarly, [20] investigated higher-order spatial phenomena and derived expressions for the effective behavior of higher-order electric and magnetic tensors.

In the present contribution, we develop a novel multiscale characterisation of an electromagnetic continuum. This approach is based on the multiscale framework cast in variational form reported in [9], called the Method of Multiscale Virtual Power (MMVP). This method relies on (i) the concept of kinematic admissibility, whereby the macro- and micro-scale primal fields are defined and linked in a physically meaningful way; (ii)

the identification of primal-dual entity pairings (power-conjugates); and (iii) the Principle of Multiscale Virtual Power, which establishes the physical connection between the macro and micro properties of the system. Importantly, this approach does not assume scale separation, as the main goal is to characterize macro-scale dual entities through the homogenisation of micro-scale phenomena in a physically consistent manner. This means that one can apply the proposed model to all frequency regimes, regardless of the composition of the micro-cell domain. Remarkably, while the homogenisation formulae of the primal entities (electric field and magnetic field) are postulated a priori, the homogenisation formulae of the dual entities (displacement field and magnetizing field) are obtained as a consequence of the Principle of Multiscale Virtual Power that governs the power exchange across scales, together with the characterisation of the micro-cell problem. Therefore, effective properties also emerge as tangent operators, which also encode the phenomena unfolding at the micro-cell level.

The MMVP has been successfully utilised in many areas of continuum mechanics, such as the modelling of inertia and body forces in solid mechanics [19], failure mechanisms in solids [37], thermoelasticity [8], second order continua [11], fluid mechanics [10], fibrous tissues [30] and materials featuring truly arbitrary micro-structure [12]. This is the first contribution to apply the MMVP in the realm of electromagnetism. The predictive and descriptive capabilities of the homogenisation approach presented in this work are tested on several cases of interest in order to validate it by comparison to established effective electromagnetic media theories. For conciseness we restrict ourselves to non-magnetic media and derive effective electromagnetic parameters in the following cases: (i) a low-frequency regime, (ii) a high-frequency regime, and (iii) a situation where the percolation phase transition occurs.

The manuscript is organised as follows. Section 2 presents the macro-scale model problem. Section 3 details the concept of kinematical admissibility through the primal homogenisation postulates. Section 4 derives the dual homogenisation formulae and the micro-cell problem by exploiting the Principle of Multiscale Virtual Power. Section 5 reports the numerical results, and Section 6 outlines the concluding remarks.

2. Macro-scale problem and duality pairings

This presentation is limited to non-magnetic materials, so Maxwell's equations are written in terms of the electric field. Therefore, let us consider a domain $\Omega \subset \mathbb{R}^3$ with boundary $\partial\Omega$, where the electric vector field $\mathbf{E}$ is defined. Maxwell's equations written in the frequency domain, and expressed in variational form read as follows: find $\mathbf{E} \in \boldsymbol{\mathcal{U}}$ such that

$$\mathcal{A}(\mathbf{E}, \hat{\mathbf{E}}) = \mathcal{L}(\hat{\mathbf{E}}) \qquad \forall \hat{\mathbf{E}} \in \boldsymbol{\mathcal{V}}, \tag{2.1}$$

where the sesquilinear form $\mathcal{A} : \boldsymbol{\mathcal{U}} \times \boldsymbol{\mathcal{V}} \mapsto \mathbb{C}$ is defined as

$$\mathcal{A}(\mathbf{E}, \hat{\mathbf{E}}) := \int_\Omega \big(\boldsymbol{\mu}_r^{-1} \operatorname{curl} \mathbf{E} \cdot \operatorname{curl} \hat{\mathbf{E}} - k_0^2 \boldsymbol{\varepsilon}_r \mathbf{E} \cdot \hat{\mathbf{E}}\big) d\Omega. \tag{2.2}$$

In addition, $\boldsymbol{\mathcal{U}}$ is a complex-valued linear manifold of admissible solutions possibly containing essential constraints, such as boundary conditions for the electric field $\mathbf{E}$, say $\overline{\mathbf{E}}$, over a portion of the boundary, say, $\partial\Omega_D$, $\boldsymbol{\mathcal{V}}$ is the complex-valued space of admissible variations of elements in $\boldsymbol{\mathcal{U}}$. We denote $\hat{(\cdot)}$ admissible variations of the field $(\cdot)$. Also, the working frequency is denoted by ω, so that $k_0 = k_0(\omega) = \omega\sqrt{\mu_0 \varepsilon_0}$, where μ_0 and ε_0 are the magnetic permeability and electric permittivity of free space. Finally, $\boldsymbol{\mu}_r$ and $\boldsymbol{\varepsilon}_r$ are second-order tensors that stand for the relative permeability and permittivity of the continuum, respectively. The right-hand side $\mathcal{L} \in \boldsymbol{\mathcal{V}}'$ may contain, in general, source terms in Ω per unit volume, say $\mathbf{Q}$, and per unit surface over a portion of the boundary,

say, $\partial\Omega_N$. These source terms, together with the essential boundary conditions in $\boldsymbol{\mathcal{U}}$ are chosen such that the existence and uniqueness of a solution for the equation (2.1) are guaranteed (see, for instance, [44]).

Note that the magnetic field $\mathbf{B}$ is related to the curl of the electric field through

$$-\boldsymbol{i}\omega\mathbf{B} = \operatorname{curl}\mathbf{E}, \tag{2.3}$$

so, hereafter, when referring to the $\operatorname{curl}\mathbf{E}$ we are equivalently referring to the magnetic field.

Standard arguments from the calculus of variations lead us to the set of partial differential equations encoded in (2.1), namely

$$\operatorname{curl}\left(\boldsymbol{\mu}_r^{-1}\operatorname{curl}\mathbf{E}\right) - k_0^2\boldsymbol{\varepsilon}_r\mathbf{E} = \mathbf{Q} \quad \text{in } \Omega, \tag{2.4}$$

endowed with proper boundary conditions [44].

Now, let us identify the dual pairings that play a role in the variational formulation (2.1). If we consider the primal fields to be the electric field $\mathbf{E}$, and its curl, $\operatorname{curl}\mathbf{E}$, then the dual vector fields are

$$\mathbf{D} = \boldsymbol{\varepsilon}_r\mathbf{E}, \tag{2.5}$$

$$\mathbf{H} = \boldsymbol{\mu}_r^{-1}\operatorname{curl}\mathbf{E}, \tag{2.6}$$

where $\mathbf{D}$ is the displacement field, and $\mathbf{H}$ is the magnetizing field (up to the scaling factor $\boldsymbol{i}\omega$). Then, we can write

$$\int_\Omega \left(\mathbf{H}\cdot\operatorname{curl}\hat{\mathbf{E}} - k_0^2\mathbf{D}\cdot\hat{\mathbf{E}}\right)d\Omega = \mathcal{L}(\hat{\mathbf{E}}) \qquad \forall\hat{\mathbf{E}}\in\boldsymbol{\mathcal{V}}. \tag{2.7}$$

In a multiscale approach, each point of the macro-scale $\mathbf{x}\in\Omega$ is linked to a micro-cell, where the electromagnetic phenomena, governed by the same fundamental principles behind (2.1), take place.

Hence, the goal of the multiscale formulation is to build a model based on micro-scale phenomena, which is capable of delivering implicit operators that replace the explicit forms of $\mathbf{D}$ and $\mathbf{H}$ defined in (2.5) and (2.6). That is, for each point $\mathbf{x}\in\Omega$, we build a formulation that implicitly defines more general operators of the form

$$\mathbf{D} = \mathcal{F}_{\mathbf{D}}(k_0(\omega), \mathbf{E}, \operatorname{curl}\mathbf{E}, \mathcal{P}_\mu), \tag{2.8}$$

$$\mathbf{H} = \mathcal{F}_{\mathbf{H}}(k_0(\omega), \mathbf{E}, \operatorname{curl}\mathbf{E}, \mathcal{P}_\mu), \tag{2.9}$$

where $\mathcal{P}_\mu$ denotes a set of parameters that characterize the micro-scale, such as the permeability and permittivity of the different phases in the micro-scale media and their topological arrangement within the micro-cell. Figure 1 schematically shows the multiscale paradigm used in this work. For each point $\mathbf{x}$ of the macro-continuum there is an associated micro-cell. The constitutive response of the micro-cell is determined by inserting the electromagnetic field $\mathbf{E}$ and $\operatorname{curl}\mathbf{E}$ and by considering some homogenisation rules for these fields. Under such hypotheses, the homogenisation of the dual entities $\mathbf{D}$ and $\mathbf{H}$ is obtained. Importantly, the dual homogenisation rules are not postulated a priori, but are derived consistently according to the hypotheses made for the primal homogenisation rules. The proposed multiscale framework is a systematic approach to model the constitutive behavior of materials with micro-structure through the characterisation of emergent properties.

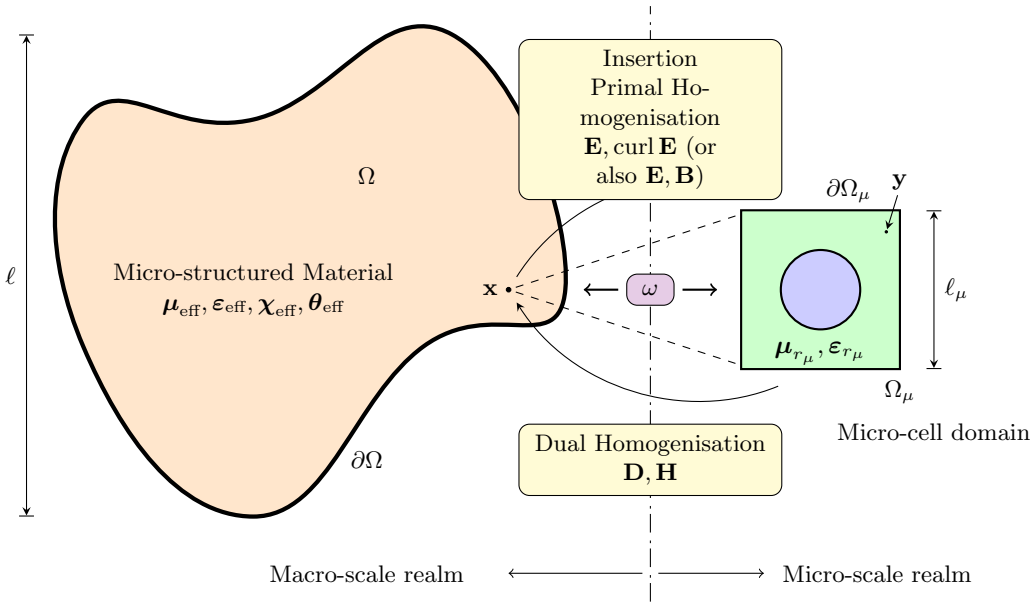

FIGURE 1. Multiscale setting for the modelling of electromagnetic micro-structured materials. For each point, $\mathbf{x}$, the electromagnetic field, $\mathbf{E}$, and its curl, $\operatorname{curl}\mathbf{E}$ (or the magnetic field $\mathbf{B}$), are inserted into the micro-cell domain, and primal homogenisation rules are hypothesized. A Principle of Multiscale Virtual Power is employed to derive the micro-cell governing problem and the dual homogenisation formulae for the dual entities $\mathbf{D}$ and $\mathbf{H}$. Material properties $\boldsymbol{\mu}_{\text{eff}}, \boldsymbol{\varepsilon}_{\text{eff}}, \boldsymbol{\chi}_{\text{eff}}, \boldsymbol{\theta}_{\text{eff}}$ naturally emerge from the formulation as tangent operators.

3. Kinematic consistency across scales

In the previous section, we presented Maxwell's equations in terms of the main primal variables, namely $\mathbf{E}$ and $\operatorname{curl}\mathbf{E}$ (or $\mathbf{B}$). These variables are the drivers of the proposed approach in the sense that, by controlling these macro-scale variables, we can perform experiments within the micro-cell and we can retrieve emergent properties from it.

3.1. **Primal variables insertion.** Consider that at each point of the macro-scale, we have the following point-wise vector fields

$$\mathbf{E}_{|\mathbf{x}} = \mathbf{E}(\mathbf{x}), \tag{3.1}$$

$$\mathbf{C}_{|\mathbf{x}} = \operatorname{curl}\mathbf{E}(\mathbf{x}). \tag{3.2}$$

Note that $\mathbf{C}$ in the expression above is related to the magnetic field $\mathbf{B}$ through (2.3), so

$$\mathbf{C}_{|\mathbf{x}} = -\boldsymbol{i}\omega\mathbf{B}_{|\mathbf{x}}. \tag{3.3}$$

These two fields are independent of each other, in the sense that we can perform admissible variations, say $\hat{\mathbf{E}}_{|\mathbf{x}}$ and $\hat{\mathbf{C}}_{|\mathbf{x}}$, in an independent manner.

Note that we can write the tensor $\nabla\mathbf{E}$ in terms of the symmetric and skew-symmetric components as $\nabla\mathbf{E} = \nabla\mathbf{E}^S + \nabla\mathbf{E}^W$, where the skew-symmetric component is linked to the curl as follows

$$\nabla\mathbf{E}^W\mathbf{w} = \frac{1}{2}\operatorname{curl}\mathbf{E} \times \mathbf{w}, \tag{3.4}$$

for any arbitrary vector $\mathbf{w}$.

Consider now a micro-scale domain, the micro-cell, denoted by $\Omega_\mu \subset \mathbb{R}^3$, with boundary $\partial\Omega_\mu$, and whose coordinates are denoted by $\mathbf{y}$. Without loss of generality, the micro-cell

is geometrically centered at the origin of the micro-scale coordinate system, such that it is satisfied

$$\int_{\Omega_\mu} \mathbf{y} d\Omega_\mu = \mathbf{0}. \tag{3.5}$$

Also, we denote by $|\Omega_\mu|$ the Lebesgue measure of Ω_μ.

At the micro-scale, we have electromagnetic phenomena driven by an electric field $\mathbf{E}_\mu$. Now, we have to define how the primal variables $\mathbf{E}_{|\mathbf{x}}$ and $\mathbf{C}_{|\mathbf{x}}$ are transferred from the macro-scale into the micro-cell. This is accomplished by expressing the micro-scale electric field in terms of these variables, through the following expansion

$$\mathbf{E}_\mu = \mathbf{E}_{|\mathbf{x}} + \nabla \mathbf{E}^W \mathbf{y} + \tilde{\mathbf{E}}_\mu, \tag{3.6}$$

which, by virtue of (3.4), can be equivalently expressed by

$$\mathbf{E}_\mu = \mathbf{E}_{|\mathbf{x}} + \frac{1}{2}\mathbf{C}_{|\mathbf{x}} \times \mathbf{y} + \tilde{\mathbf{E}}_\mu. \tag{3.7}$$

Note that in this expansion we are only concerned with the skew-symmetric part of the first-order gradient because it is the component of the gradient that exerts power at the macro-scale. Therefore, it is the only term we are interested in controlling at the micro-scale. In the above, the vector field $\tilde{\mathbf{E}}_\mu$ represents the high-order fluctuations of the electric field at the micro-scale.

3.2. **Primal variables homogenisation.** Following the concept of kinematical admissibility proposed in [9], we now define admissible macro-scale and micro-scale fields as those that satisfy certain rules of scale transfer. The following hypotheses shape the primal scale information transfer between the electric field and its (skew-symmetric component of the) gradient at point $\mathbf{x}$, and the corresponding micro-scale fields defined within the associated micro-cell. First, we consider that the electric field in the micro-cell has to be, on average, equal to the macro-scale electric field

$$\mathbf{E}_{|\mathbf{x}} = \frac{1}{|\Omega_\mu|} \int_{\Omega_\mu} \mathbf{E}_\mu d\Omega_\mu. \tag{3.8}$$

Second, we consider that the skew-symmetric component of the gradient of the electric field in the micro-scale has to equal the macro-scale skew-symmetric component of the electric field gradient, that is

$$(\nabla \mathbf{E})^W_{|\mathbf{x}} = \frac{1}{|\Omega_\mu|} \int_{\Omega_\mu} (\nabla_{\mathbf{y}} \mathbf{E}_\mu)^W d\Omega_\mu. \tag{3.9}$$

Exploiting the relation (3.4), expression (3.9) can be equivalently written as

$$\mathbf{C}_{|\mathbf{x}} = \frac{1}{|\Omega_\mu|} \int_{\Omega_\mu} \mathrm{curl}_{\mathbf{y}}\, \mathbf{E}_\mu d\Omega_\mu. \tag{3.10}$$

Expressions (3.8) and (3.10) are the fundamental constraints that define the concept of admissibility of the triple $(\mathbf{E}_{|\mathbf{x}}, \mathbf{C}_{|\mathbf{x}}, \mathbf{E}_\mu)$. Introducing expansion (3.7) into (3.8) yields

$$\mathbf{E}_{|\mathbf{x}} = \frac{1}{|\Omega_\mu|} \int_{\Omega_\mu} \left(\mathbf{E}_{|\mathbf{x}} + \frac{1}{2}\mathbf{C}_{|\mathbf{x}} \times \mathbf{y} + \tilde{\mathbf{E}}_\mu \right) d\Omega_\mu. \tag{3.11}$$

Taking into account (3.5), we get

$$\int_{\Omega_\mu} \tilde{\mathbf{E}}_\mu d\Omega_\mu = \mathbf{0}. \tag{3.12}$$

Now, introducing (3.7) into (3.10) we write

$$\mathbf{C}_{|\mathbf{x}} = \frac{1}{|\Omega_\mu|}\int_{\Omega_\mu} \mathrm{curl}_{\mathbf{y}} \left(\mathbf{E}_{|\mathbf{x}} + \frac{1}{2}\mathbf{C}_{|\mathbf{x}} \times \mathbf{y} + \tilde{\mathbf{E}}_\mu \right) d\Omega_\mu. \tag{3.13}$$

Again, considering (3.5), and the fact that $\mathrm{curl}_{\mathbf{y}}(\mathbf{V} \times \mathbf{y}) = 2\mathbf{V}$, for any constant vector $\mathbf{V} \in \mathbb{C}^3$, we get

$$\int_{\Omega_\mu} \mathrm{curl}_{\mathbf{y}}\, \tilde{\mathbf{E}}_\mu d\Omega_\mu = \mathbf{0}. \tag{3.14}$$

Applying the Gauss' theorem to this case, we obtain the following constraint over the electric fluctuation field

$$\int_{\partial\Omega_\mu} \mathbf{n}_\mu \times \tilde{\mathbf{E}}_\mu d\partial\Omega_\mu = \mathbf{0}, \tag{3.15}$$

where $\mathbf{n}_\mu$ is the unit outward vector to the boundary $\partial\Omega_\mu$.

3.3. **Primal variables admissibility.** We say that the triple $(\mathbf{E}_{|\mathbf{x}}, \mathbf{C}_{|\mathbf{x}}, \mathbf{E}_\mu)$ is admissible if, given $\mathbf{E}_{|\mathbf{x}} \in \mathbb{C}^3$ and $\mathbf{C}_{|\mathbf{x}} \in \mathbb{C}^3$, the fluctuation field satisfies (3.12) and (3.15). Therefore, we define the set (actually a space) of admissible fluctuation fields as follows

$$\tilde{\boldsymbol{\mathcal{V}}}_\mu = \left\{ \tilde{\mathbf{E}}_\mu \in \mathbf{H}_{\mathrm{curl}}(\Omega_\mu) : \int_{\Omega_\mu} \tilde{\mathbf{E}}_\mu d\Omega_\mu = \mathbf{0},\ \int_{\partial\Omega_\mu} \mathbf{n}_\mu \times \tilde{\mathbf{E}}_\mu d\partial\Omega_\mu = \mathbf{0} \right\}, \tag{3.16}$$

where $\mathbf{H}_{\mathrm{curl}}(\Omega_\mu)$ is the complex-valued space of square integrable vector fields in Ω_μ with square integrable curl in Ω_μ.

Note that any subspace $\tilde{\boldsymbol{\mathcal{V}}}_\mu^X \subset \tilde{\boldsymbol{\mathcal{V}}}_\mu$ can be considered as space of admissible fluctuation fields, and this is why space $\tilde{\boldsymbol{\mathcal{V}}}_\mu$ is called the space of minimally constrained fluctuation fields. Alternative subspaces can be the so-called linear subspace, defined as

$$\tilde{\boldsymbol{\mathcal{V}}}_\mu^L = \left\{ \tilde{\mathbf{E}}_\mu \in \mathbf{H}_{\mathrm{curl}}(\Omega_\mu) : \int_{\Omega_\mu} \tilde{\mathbf{E}}_\mu d\Omega_\mu = \mathbf{0},\ \tilde{\mathbf{E}}_\mu|_{\partial\Omega_\mu} = \mathbf{0} \right\}, \tag{3.17}$$

and the periodic subspace, defined by partitioning the boundary $\partial\Omega_\mu$ into opposing parts $\partial\Omega_\mu^+$ and $\partial\Omega_\mu^-$ for which we have $\mathbf{n}_\mu|_{\partial\Omega_\mu^+} = -\mathbf{n}_\mu|_{\partial\Omega_\mu^-}$

$$\tilde{\boldsymbol{\mathcal{V}}}_\mu^P = \left\{ \tilde{\mathbf{E}}_\mu \in \mathbf{H}_{\mathrm{curl}}(\Omega_\mu) : \int_{\Omega_\mu} \tilde{\mathbf{E}}_\mu d\Omega_\mu = \mathbf{0},\ \tilde{\mathbf{E}}_\mu|_{\partial\Omega_\mu^+} = \tilde{\mathbf{E}}_\mu|_{\partial\Omega_\mu^-} \right\}. \tag{3.18}$$

Clearly, we have $\tilde{\boldsymbol{\mathcal{V}}}_\mu^L \subset \tilde{\boldsymbol{\mathcal{V}}}_\mu^P \subset \tilde{\boldsymbol{\mathcal{V}}}_\mu$.

4. Energetic consistency across scales

After having defined the primal variables insertion and concept of admissibility of macro- and micro-scale fields, the next step consists of introducing the physical connection between the scales through the Principle of Multiscale Virtual Power, as established by the Method of Multiscale Virtual Power [9]. From this principle, we define the dual homogenisation formulae that characterize the emergent properties of the micro-structured material and also the micro-cell problem that closes such a characterisation.

4.1. **Principle of Multiscale Virtual Power.** By inspecting (2.7), we can define the total virtual power per unit volume at the point $\mathbf{x} \in \Omega$, i.e. at the macro-scale, as follows

$$P^{\mathbf{x}}_{\text{tot}}(\hat{\mathbf{E}}_{|\mathbf{x}}, \hat{\mathbf{C}}_{|\mathbf{x}}) = (\mathbf{H} \cdot \hat{\mathbf{C}} - k_0^2 \mathbf{D} \cdot \hat{\mathbf{E}})_{|\mathbf{x}}. \tag{4.1}$$

In turn, we define the total virtual power per unit volume at the micro-scale as follows

$$P^{\mu}_{\text{tot}}(\hat{\mathbf{E}}_{\mu}) = \frac{1}{|\Omega_\mu|} \int_{\Omega_\mu} \big(\boldsymbol{\mu}^{-1}_{r_\mu} \operatorname{curl}_{\mathbf{y}} \mathbf{E}_\mu \cdot \operatorname{curl}_{\mathbf{y}} \hat{\mathbf{E}}_\mu - k_0^2 \boldsymbol{\varepsilon}_{r_\mu} \mathbf{E}_\mu \cdot \hat{\mathbf{E}}_\mu \big) d\Omega_\mu, \tag{4.2}$$

where $\boldsymbol{\mu}_{r_\mu}$ and $\boldsymbol{\varepsilon}_{r_\mu}$ are, respectively, the second-order permeability and permittivity tensors of the phases that characterize the micro-cell continuum.

Now, we establish the hypothesis that is concerned with the transfer of power between scales. We postulate that the total power per unit volume at $\mathbf{x}$ from the macro-scale must be equal to the same quantity defined within the associated micro-cell for all admissible fields $(\hat{\mathbf{E}}_{|\mathbf{x}}, \hat{\mathbf{C}}_{|\mathbf{x}}, \hat{\mathbf{E}}_\mu)$. This previous statement is the Principle of Multiscale Virtual Power [9], which in variational form reads

$$P^{\mathbf{x}}_{\text{tot}}(\hat{\mathbf{E}}_{|\mathbf{x}}, \hat{\mathbf{C}}_{|\mathbf{x}}) = P^{\mu}_{\text{tot}}(\hat{\mathbf{E}}_{\mu}) \qquad \forall (\hat{\mathbf{E}}_{|\mathbf{x}}, \hat{\mathbf{C}}_{|\mathbf{x}}, \hat{\mathbf{E}}_\mu) \text{ admissible}, \tag{4.3}$$

that is

$$(\mathbf{H} \cdot \hat{\mathbf{C}} - k_0^2 \mathbf{D} \cdot \hat{\mathbf{E}})_{|\mathbf{x}} = \frac{1}{|\Omega_\mu|} \int_{\Omega_\mu} \big(\boldsymbol{\mu}^{-1}_{r_\mu} \operatorname{curl}_{\mathbf{y}} \mathbf{E}_\mu \cdot \operatorname{curl}_{\mathbf{y}} \hat{\mathbf{E}}_\mu - k_0^2 \boldsymbol{\varepsilon}_{r_\mu} \mathbf{E}_\mu \cdot \hat{\mathbf{E}}_\mu \big) d\Omega_\mu$$
$$\forall (\hat{\mathbf{E}}_{|\mathbf{x}}, \hat{\mathbf{C}}_{|\mathbf{x}}, \hat{\mathbf{E}}_\mu) \text{ admissible}. \tag{4.4}$$

Let us rewrite the problem in terms of the fluctuation field $\tilde{\mathbf{E}}_\mu$. To do so, we introduce the expansion (3.7) for $\mathbf{E}_\mu$ and its variation $\hat{\mathbf{E}}_\mu$ into the previous expression

$$\begin{aligned}
&(\mathbf{H} \cdot \hat{\mathbf{C}} - k_0^2 \mathbf{D} \cdot \hat{\mathbf{E}})_{|\mathbf{x}} = \\
&\quad \frac{1}{|\Omega_\mu|} \int_{\Omega_\mu} \Bigg[\boldsymbol{\mu}^{-1}_{r_\mu} \operatorname{curl}_{\mathbf{y}} \left(\mathbf{E}_{|\mathbf{x}} + \frac{1}{2} \mathbf{C}_{|\mathbf{x}} \times \mathbf{y} + \tilde{\mathbf{E}}_\mu \right) \cdot \operatorname{curl}_{\mathbf{y}} \left(\hat{\mathbf{E}}_{|\mathbf{x}} + \frac{1}{2} \hat{\mathbf{C}}_{|\mathbf{x}} \times \mathbf{y} + \hat{\tilde{\mathbf{E}}}_\mu \right) \\
&\qquad - k_0^2 \boldsymbol{\varepsilon}_{r_\mu} \left(\mathbf{E}_{|\mathbf{x}} + \frac{1}{2} \mathbf{C}_{|\mathbf{x}} \times \mathbf{y} + \tilde{\mathbf{E}}_\mu \right) \cdot \left(\hat{\mathbf{E}}_{|\mathbf{x}} + \frac{1}{2} \hat{\mathbf{C}}_{|\mathbf{x}} \times \mathbf{y} + \hat{\tilde{\mathbf{E}}}_\mu \right) \Bigg] d\Omega_\mu \\
&\qquad\qquad \forall (\hat{\mathbf{E}}_{|\mathbf{x}}, \hat{\mathbf{C}}_{|\mathbf{x}}, \hat{\tilde{\mathbf{E}}}_\mu) \in \mathbb{C}^3 \times \mathbb{C}^3 \times \tilde{\boldsymbol{\mathcal{V}}}_\mu.
\end{aligned} \tag{4.5}$$

The advantage of expression (4.5) is that all the fields in the triple $(\hat{\mathbf{E}}_{|\mathbf{x}}, \hat{\mathbf{C}}_{|\mathbf{x}}, \hat{\tilde{\mathbf{E}}}_\mu)$ are independent of each other, and this will facilitate the derivation of the homogenisation formulae and of the micro-cell equilibrium problem in the next sections.

In expression (4.5), the space $\tilde{\boldsymbol{\mathcal{V}}}_\mu$ is the minimally constrained space of admissible variations defined in (3.16), as well as any subspace of it.

4.2. **Dual homogenisation formulae.** Let us first consider that $(\hat{\mathbf{E}}_{|\mathbf{x}}, \hat{\mathbf{C}}_{|\mathbf{x}}, \hat{\tilde{\mathbf{E}}}_\mu) = (\hat{\mathbf{E}}_{|\mathbf{x}}, \mathbf{0}, \mathbf{0})$, so, from (4.5) we obtain

$$-k_0^2 (\mathbf{D} \cdot \hat{\mathbf{E}})_{|\mathbf{x}} = -\frac{1}{|\Omega_\mu|} \int_{\Omega_\mu} k_0^2 \boldsymbol{\varepsilon}_{r_\mu} \left(\mathbf{E}_{|\mathbf{x}} + \frac{1}{2} \mathbf{C}_{|\mathbf{x}} \times \mathbf{y} + \tilde{\mathbf{E}}_\mu \right) \cdot \hat{\mathbf{E}}_{|\mathbf{x}} d\Omega_\mu \quad \forall \hat{\mathbf{E}}_{|\mathbf{x}} \in \mathbb{C}^3. \tag{4.6}$$

Therefore, it must necessarily be

$$\mathbf{D}_{|\mathbf{x}} = \frac{1}{|\Omega_\mu|} \int_{\Omega_\mu} \boldsymbol{\varepsilon}_{r_\mu} \left(\mathbf{E}_{|\mathbf{x}} + \frac{1}{2} \mathbf{C}_{|\mathbf{x}} \times \mathbf{y} + \tilde{\mathbf{E}}_\mu \right) d\Omega_\mu. \tag{4.7}$$

The expression (4.7) yields the variationally consistent rule to derive the homogenised behavior of the displacement vector $\mathbf{D}$ in terms of the micro-scale phenomena. Observe that due to the presence of the fluctuation field, this response is frequency-dependent.

Second, let us consider that $(\hat{\mathbf{E}}_{|\mathbf{x}}, \hat{\mathbf{C}}_{|\mathbf{x}}, \hat{\tilde{\mathbf{E}}}_\mu) = (\mathbf{0}, \hat{\mathbf{C}}_{|\mathbf{x}}, \mathbf{0})$, so, from (4.5) we get

$$(\mathbf{H}\cdot\hat{\mathbf{C}})_{|\mathbf{x}} = \frac{1}{|\Omega_\mu|}\int_{\Omega_\mu}\Bigg[\boldsymbol{\mu}_{r_\mu}^{-1}\,\mathrm{curl}_{\mathbf{y}}\left(\mathbf{E}_{|\mathbf{x}} + \frac{1}{2}\mathbf{C}_{|\mathbf{x}}\times\mathbf{y} + \tilde{\mathbf{E}}_\mu\right)\cdot\mathrm{curl}_{\mathbf{y}}\left(\frac{1}{2}\hat{\mathbf{C}}_{|\mathbf{x}}\times\mathbf{y}\right)$$
$$- k_0^2\boldsymbol{\varepsilon}_{r_\mu}\left(\mathbf{E}_{|\mathbf{x}} + \frac{1}{2}\mathbf{C}_{|\mathbf{x}}\times\mathbf{y} + \tilde{\mathbf{E}}_\mu\right)\cdot\left(\frac{1}{2}\hat{\mathbf{C}}_{|\mathbf{x}}\times\mathbf{y}\right)\Bigg]d\Omega_\mu \qquad \forall\hat{\mathbf{C}}_{|\mathbf{x}}\in\mathbb{C}^3. \quad (4.8)$$

Using identities (A.1) and (A.2) (see A), we get

$$(\mathbf{H}\cdot\hat{\mathbf{C}})_{|\mathbf{x}} = \frac{1}{|\Omega_\mu|}\int_{\Omega_\mu}\Bigg[\boldsymbol{\mu}_{r_\mu}^{-1}\big(\mathbf{C}_{|\mathbf{x}} + \mathrm{curl}_{\mathbf{y}}\,\tilde{\mathbf{E}}_\mu\big)\cdot\hat{\mathbf{C}}_{|\mathbf{x}}$$
$$- k_0^2\frac{\mathbf{y}}{2}\times\boldsymbol{\varepsilon}_{r_\mu}\left(\mathbf{E}_{|\mathbf{x}} + \frac{1}{2}\mathbf{C}_{|\mathbf{x}}\times\mathbf{y} + \tilde{\mathbf{E}}_\mu\right)\cdot\hat{\mathbf{C}}_{|\mathbf{x}}\Bigg]d\Omega_\mu \qquad \forall\hat{\mathbf{C}}_{|\mathbf{x}}\in\mathbb{C}^3. \quad (4.9)$$

Therefore, it must necessarily be

$$\mathbf{H}_{|\mathbf{x}} = \frac{1}{|\Omega_\mu|}\int_{\Omega_\mu}\left[\boldsymbol{\mu}_{r_\mu}^{-1}\big(\mathbf{C}_{|\mathbf{x}} + \mathrm{curl}_{\mathbf{y}}\,\tilde{\mathbf{E}}_\mu\big) - \frac{1}{2}k_0^2\,\mathbf{y}\times\boldsymbol{\varepsilon}_{r_\mu}\left(\mathbf{E}_{|\mathbf{x}} + \frac{1}{2}\mathbf{C}_{|\mathbf{x}}\times\mathbf{y} + \tilde{\mathbf{E}}_\mu\right)\right]d\Omega_\mu. \quad (4.10)$$

The expression (4.10) yields the homogenisation formula to retrieve the magnetizing field $\mathbf{H}$ from the phenomena that take place in the micro-scale domain. Note that this response is frequency-dependent, both explicitly because of the presence of k_0, and implicitly because of the presence of the fluctuation field.

4.3. **Micro-cell problem.** Finally, consider $(\hat{\mathbf{E}}_{|\mathbf{x}}, \hat{\mathbf{C}}_{|\mathbf{x}}, \hat{\tilde{\mathbf{E}}}_\mu) = (\mathbf{0}, \mathbf{0}, \hat{\mathbf{E}}_\mu)$, hence, from (4.5) it results

$$\int_{\Omega_\mu}\Bigg[\boldsymbol{\mu}_{r_\mu}^{-1}\big(\mathbf{C}_{|\mathbf{x}} + \mathrm{curl}_{\mathbf{y}}\,\tilde{\mathbf{E}}_\mu\big)\cdot\mathrm{curl}_{\mathbf{y}}\,\hat{\tilde{\mathbf{E}}}_\mu$$
$$- k_0^2\boldsymbol{\varepsilon}_{r_\mu}\left(\mathbf{E}_{|\mathbf{x}} + \frac{1}{2}\mathbf{C}_{|\mathbf{x}}\times\mathbf{y} + \tilde{\mathbf{E}}_\mu\right)\cdot\hat{\tilde{\mathbf{E}}}_\mu\Bigg]d\Omega_\mu = 0 \qquad \forall\hat{\tilde{\mathbf{E}}}_\mu\in\tilde{\boldsymbol{\mathcal{V}}}_\mu. \quad (4.11)$$

This variational problem (4.11) gives the full characterisation of the fluctuation field $\tilde{\mathbf{E}}_\mu$ for given macro-scale quantities $(\mathbf{E}_{|\mathbf{x}}, \mathbf{C}_{|\mathbf{x}})$. That is, it characterizes an operator of the form

$$\begin{aligned}\mathcal{M}_\mu : \mathbb{C}^3\times\mathbb{C}^3 &\to \tilde{\boldsymbol{\mathcal{V}}}_\mu,\\ (\mathbf{E}_{|\mathbf{x}}, \mathbf{C}_{|\mathbf{x}}) &\mapsto \mathcal{M}_\mu(\mathbf{E}_{|\mathbf{x}}, \mathbf{C}_{|\mathbf{x}}) = \tilde{\mathbf{E}}_\mu.\end{aligned} \quad (4.12)$$

The multiscale procedure to explicitly compute the pair $(\mathbf{D}_{|\mathbf{x}}, \mathbf{H}_{|\mathbf{x}})$ reads as follows:

(1) Given the pair $(\mathbf{E}_{|\mathbf{x}}, \mathbf{C}_{|\mathbf{x}})$, obtain $\tilde{\mathbf{E}}_\mu$ by solving the variational problem (4.11).
(2) Given the pair $(\mathbf{E}_{|\mathbf{x}}, \mathbf{C}_{|\mathbf{x}})$, and the field $\tilde{\mathbf{E}}_\mu$ obtained in step 1, compute $\mathbf{D}_{|\mathbf{x}}$ using (4.7).
(3) Given the pair $(\mathbf{E}_{|\mathbf{x}}, \mathbf{C}_{|\mathbf{x}})$, and the field $\tilde{\mathbf{E}}_\mu$ obtained in step 1, compute $\mathbf{H}_{|\mathbf{x}}$ using (4.10).

It is important to recall that any subspace $\tilde{\boldsymbol{\mathcal{V}}}_\mu^X \subset \tilde{\boldsymbol{\mathcal{V}}}_\mu$ also yields a valid multiscale model. Different subspaces will result in different model predictions, as these subspaces encompass the assumptions of the interaction between the micro-cell and the neighboring continuum.

4.4. **Tangent operators.** Note that in a fully coupled multiscale problem, the pair $(\mathbf{E}_{|\mathbf{x}}, \mathbf{C}_{|\mathbf{x}})$ is unknown, and some linearisation procedure must be applied to address the nonlinearity posed by the implicit coupling between the scales. A linearisation procedure is also required to understand the potential of the formulation in terms of predicted effective material properties, such as effective permeability and permittivity, for example.

From the variational problem (2.7), we note that the nonlinearities are present in the relation between the homogenised quantities $(\mathbf{D}_{|\mathbf{x}}, \mathbf{H}_{|\mathbf{x}})$ and the variables $(\mathbf{E}_{|\mathbf{x}}, \mathbf{C}_{|\mathbf{x}})$, as dictated by expressions (4.7) and (4.10) (nonlinearities are implicit in the fluctuation field $\tilde{\mathbf{E}}_\mu$). The linearised version of the macro-scale variational equation (2.7), reads

$$\int_\Omega \big([\mathcal{D}_{\mathbf{E}}\mathbf{H}]\mathbf{E}\cdot\operatorname{curl}\hat{\mathbf{E}} + [\mathcal{D}_{\mathbf{C}}\mathbf{H}]\operatorname{curl}\mathbf{E}\cdot\operatorname{curl}\hat{\mathbf{E}} - k_0^2[\mathcal{D}_{\mathbf{E}}\mathbf{D}]\mathbf{E}\cdot\hat{\mathbf{E}} - k_0^2[\mathcal{D}_{\mathbf{C}}\mathbf{D}]\operatorname{curl}\mathbf{E}\cdot\hat{\mathbf{E}}\big)d\Omega = \mathcal{R}(\hat{\mathbf{E}}) \qquad \forall\hat{\mathbf{E}}\in\boldsymbol{\mathcal{V}}. \quad (4.13)$$

where $\mathcal{R}(\hat{\mathbf{E}})$ stands for the residual of (2.7). Most importantly, $[\mathcal{D}_{\mathbf{E}}\mathbf{H}]$ and $[\mathcal{D}_{\mathbf{C}}\mathbf{H}]$ are the tangent relations between $\mathbf{H}$ and the primal variables $\mathbf{E}$ and $\mathbf{C}=\operatorname{curl}\mathbf{E}$, respectively, and $[\mathcal{D}_{\mathbf{E}}\mathbf{D}]$ and $[\mathcal{D}_{\mathbf{C}}\mathbf{D}]$ are the corresponding tangent relations between $\mathbf{D}$ and the same primal variables.

The first $[\mathcal{D}_{\mathbf{E}}\mathbf{H}]$ and the fourth $[\mathcal{D}_{\mathbf{C}}\mathbf{D}]$ tangent tensors are non-conventional terms that emerge from the interaction of micro-scale phenomena. The second $[\mathcal{D}_{\mathbf{C}}\mathbf{H}]$ and the third $[\mathcal{D}_{\mathbf{E}}\mathbf{D}]$ tangent tensors are related to the effective permeability $\boldsymbol{\mu}_{\text{eff}}$ and permittivity $\boldsymbol{\varepsilon}_{\text{eff}}$, respectively.

Let us introduce the following notations for all the second-order tensors that appear in (4.13)

$$\boldsymbol{\mu}_{\text{eff}}^{-1} := [\mathcal{D}_{\mathbf{C}}\mathbf{H}], \quad \boldsymbol{\varepsilon}_{\text{eff}} := [\mathcal{D}_{\mathbf{E}}\mathbf{D}], \quad \boldsymbol{\chi}_{\text{eff}} := [\mathcal{D}_{\mathbf{E}}\mathbf{H}], \quad \boldsymbol{\theta}_{\text{eff}} := [\mathcal{D}_{\mathbf{C}}\mathbf{D}], \quad (4.14)$$

Hence, after rearranging terms, equation (4.13) becomes

$$\int_\Omega \big(\boldsymbol{\mu}_{\text{eff}}^{-1}\operatorname{curl}\mathbf{E}\cdot\operatorname{curl}\hat{\mathbf{E}} - k_0^2\boldsymbol{\varepsilon}_{\text{eff}}\mathbf{E}\cdot\hat{\mathbf{E}} + \boldsymbol{\chi}_{\text{eff}}\mathbf{E}\cdot\operatorname{curl}\hat{\mathbf{E}} - k_0^2\boldsymbol{\theta}_{\text{eff}}\operatorname{curl}\mathbf{E}\cdot\hat{\mathbf{E}}\big)d\Omega = \mathcal{R}(\hat{\mathbf{E}}) \qquad \forall\hat{\mathbf{E}}\in\boldsymbol{\mathcal{V}}. \quad (4.15)$$

The full linearisation procedure is presented in B, which yields the characterisation of the tangent operators appearing in (4.14), that is

$$\boldsymbol{\mu}_{\text{eff}}^{-1} := \frac{1}{|\Omega_\mu|}\int_{\Omega_\mu}\left[\boldsymbol{\mu}_{r_\mu}^{-1}(\mathbf{I}+\operatorname{curl}_{\mathbf{y}}\mathbf{M}_{\mathbf{C}}) - \frac{1}{2}k_0^2[\mathbf{y}]_\times\boldsymbol{\varepsilon}_{r_\mu}\left(\frac{1}{2}[\mathbf{y}]_\times^T + \mathbf{M}_{\mathbf{C}}\right)\right]d\Omega_\mu, \quad (4.16)$$

$$\boldsymbol{\varepsilon}_{\text{eff}} := \frac{1}{|\Omega_\mu|}\int_{\Omega_\mu}\boldsymbol{\varepsilon}_{r_\mu}\big(\mathbf{I}+\mathbf{M}_{\mathbf{E}}\big)d\Omega_\mu, \quad (4.17)$$

$$\boldsymbol{\chi}_{\text{eff}} := \frac{1}{|\Omega_\mu|}\int_{\Omega_\mu}\left[-\frac{1}{2}k_0^2[\mathbf{y}]_\times\boldsymbol{\varepsilon}_{r_\mu}(\mathbf{I}+\mathbf{M}_{\mathbf{E}}) + \boldsymbol{\mu}_{r_\mu}^{-1}\operatorname{curl}_{\mathbf{y}}\mathbf{M}_{\mathbf{E}}\right]d\Omega_\mu, \quad (4.18)$$

$$\boldsymbol{\theta}_{\text{eff}} := \frac{1}{|\Omega_\mu|}\int_{\Omega_\mu}\boldsymbol{\varepsilon}_{r_\mu}\left(\frac{1}{2}[\mathbf{y}]_\times^\top + \mathbf{M}_{\mathbf{C}}\right)d\Omega_\mu. \quad (4.19)$$

In the expressions above, the second-order tensors $\mathbf{M}_{\mathbf{E}}$ and $\mathbf{M}_{\mathbf{C}}$ are, respectively, defined by

$$\mathbf{M}_{\mathbf{E}} = [\mathbf{U}_\mu^{(j)}]_i\,(\mathbf{e}_i\otimes\mathbf{e}_j), \quad (4.20)$$

$$\mathbf{M}_{\mathbf{C}} = [\mathbf{V}_\mu^{(j)}]_i\,(\mathbf{e}_i\otimes\mathbf{e}_j), \quad (4.21)$$

where $\mathbf{U}_\mu^{(i)} \in \tilde{\boldsymbol{\mathcal{V}}}_\mu$, $i = 1, 2, 3$, are the solutions to the set of canonical problems

$$\int_{\Omega_\mu} \big(\boldsymbol{\mu}_{r_\mu}^{-1} \operatorname{curl}_{\mathbf{y}} \mathbf{U}_\mu^{(i)} \cdot \operatorname{curl}_{\mathbf{y}} \hat{\tilde{\mathbf{E}}}_\mu - k_0^2 \boldsymbol{\varepsilon}_{r_\mu} \mathbf{U}_\mu^{(i)} \cdot \hat{\tilde{\mathbf{E}}}_\mu\big) d\Omega_\mu = \int_{\Omega_\mu} k_0^2 \boldsymbol{\varepsilon}_{r_\mu} \mathbf{e}_i \cdot \hat{\tilde{\mathbf{E}}}_\mu d\Omega_\mu \quad \forall \hat{\tilde{\mathbf{E}}}_\mu \in \tilde{\boldsymbol{\mathcal{V}}}_\mu. \tag{4.22}$$

whereas $\mathbf{V}_\mu^{(i)} \in \tilde{\boldsymbol{\mathcal{V}}}_\mu$, $i = 1, 2, 3$, are the solutions to the canonical problems

$$\int_{\Omega_\mu} \big(\boldsymbol{\mu}_{r_\mu}^{-1} \operatorname{curl}_{\mathbf{y}} \mathbf{V}_\mu^{(i)} \cdot \operatorname{curl}_{\mathbf{y}} \hat{\tilde{\mathbf{E}}}_\mu - k_0^2 \boldsymbol{\varepsilon}_{r_\mu} \mathbf{V}_\mu^{(i)} \cdot \hat{\tilde{\mathbf{E}}}_\mu\big) d\Omega_\mu =$$
$$- \int_{\Omega_\mu} \left[\boldsymbol{\mu}_{r_\mu}^{-1} \mathbf{e}_i \cdot \operatorname{curl}_{\mathbf{y}} \hat{\tilde{\mathbf{E}}}_\mu - \frac{1}{2} k_0^2 \boldsymbol{\varepsilon}_{r_\mu} (\mathbf{e}_i \times \mathbf{y}) \cdot \hat{\tilde{\mathbf{E}}}_\mu\right] d\Omega_\mu \quad \forall \hat{\tilde{\mathbf{E}}}_\mu \in \tilde{\boldsymbol{\mathcal{V}}}_\mu. \tag{4.23}$$

See B for the full details.

4.5. **Connection to higher-order theories of electromagnetism.** Consider again the variational equation (4.15) and the definitions of the effective properties (4.16)-(4.19). The expressions of $\mathbf{M_E}$ and $\mathbf{M_C}$ defined in (4.20) and (4.21) can be equivalently characterised as follows

$$\mathbf{M_E} = k_0^2 \mathbf{M_E^0} = k_0^2 [\mathbf{U}_{\mu,0}^{(j)}]_i \, (\mathbf{e}_i \otimes \mathbf{e}_j), \tag{4.24}$$
$$\mathbf{M_C} = \mathbf{M_C^0} - k_0^2 \mathbf{M_C^1} = [\mathbf{V}_{\mu,0}^{(j)}]_i \, (\mathbf{e}_i \otimes \mathbf{e}_j) - k_0^2 [\mathbf{V}_{\mu,1}^{(j)}]_i \, (\mathbf{e}_i \otimes \mathbf{e}_j), \tag{4.25}$$

where $\mathbf{U}_{\mu,0}^{(i)} \in \tilde{\boldsymbol{\mathcal{V}}}_\mu$, $i = 1, 2, 3$, are the solutions to the set of canonical problems (note the difference in the right-hand side with (4.22))

$$\int_{\Omega_\mu} \big(\boldsymbol{\mu}_{r_\mu}^{-1} \operatorname{curl}_{\mathbf{y}} \mathbf{U}_{\mu,0}^{(i)} \cdot \operatorname{curl}_{\mathbf{y}} \hat{\tilde{\mathbf{E}}}_\mu - k_0^2 \boldsymbol{\varepsilon}_{r_\mu} \mathbf{U}_{\mu,0}^{(i)} \cdot \hat{\tilde{\mathbf{E}}}_\mu\big) d\Omega_\mu = \int_{\Omega_\mu} \boldsymbol{\varepsilon}_{r_\mu} \mathbf{e}_i \cdot \hat{\tilde{\mathbf{E}}}_\mu d\Omega_\mu \quad \forall \hat{\tilde{\mathbf{E}}}_\mu \in \tilde{\boldsymbol{\mathcal{V}}}_\mu. \tag{4.26}$$

whereas $\mathbf{V}_{\mu,0}^{(i)} \in \tilde{\boldsymbol{\mathcal{V}}}_\mu$, $i = 1, 2, 3$, are the solutions to the canonical problems (take into account the first term in the right-hand side of (4.23))

$$\int_{\Omega_\mu} \big(\boldsymbol{\mu}_{r_\mu}^{-1} \operatorname{curl}_{\mathbf{y}} \mathbf{V}_{\mu,0}^{(i)} \cdot \operatorname{curl}_{\mathbf{y}} \hat{\tilde{\mathbf{E}}}_\mu - k_0^2 \boldsymbol{\varepsilon}_{r_\mu} \mathbf{V}_{\mu,0}^{(i)} \cdot \hat{\tilde{\mathbf{E}}}_\mu\big) d\Omega_\mu =$$
$$- \int_{\Omega_\mu} \boldsymbol{\mu}_{r_\mu}^{-1} \mathbf{e}_i \cdot \operatorname{curl}_{\mathbf{y}} \hat{\tilde{\mathbf{E}}}_\mu d\Omega_\mu \quad \forall \hat{\tilde{\mathbf{E}}}_\mu \in \tilde{\boldsymbol{\mathcal{V}}}_\mu. \tag{4.27}$$

and $\mathbf{V}_{\mu,1}^{(i)} \in \tilde{\boldsymbol{\mathcal{V}}}_\mu$, $i = 1, 2, 3$, are the solutions to the canonical problems (take into account the second term -times a constant- in the right-hand side of (4.23))

$$\int_{\Omega_\mu} \big(\boldsymbol{\mu}_{r_\mu}^{-1} \operatorname{curl}_{\mathbf{y}} \mathbf{V}_{\mu,1}^{(i)} \cdot \operatorname{curl}_{\mathbf{y}} \hat{\tilde{\mathbf{E}}}_\mu - k_0^2 \boldsymbol{\varepsilon}_{r_\mu} \mathbf{V}_{\mu,1}^{(i)} \cdot \hat{\tilde{\mathbf{E}}}_\mu\big) d\Omega_\mu =$$
$$- \frac{1}{2} \int_{\Omega_\mu} \boldsymbol{\varepsilon}_{r_\mu} (\mathbf{e}_i \times \mathbf{y}) \cdot \hat{\tilde{\mathbf{E}}}_\mu d\Omega_\mu \quad \forall \hat{\tilde{\mathbf{E}}}_\mu \in \tilde{\boldsymbol{\mathcal{V}}}_\mu. \tag{4.28}$$

Let us rewrite the effective properties (4.16)-(4.19), now introducing (4.24) and (4.25). Then, the characterisation of the effective properties in terms of the powers of k_0 is the

following

$$\boldsymbol{\mu}_{\text{eff}}^{-1} := \frac{1}{|\Omega_\mu|}\int_{\Omega_\mu}\left[\boldsymbol{\mu}_{r_\mu}^{-1}(\mathbf{I}+\text{curl}_{\mathbf{y}}(\mathbf{M}_{\mathbf{C}}^0-k_0^2\mathbf{M}_{\mathbf{C}}^1))-\frac{1}{2}k_0^2[\mathbf{y}]_\times\boldsymbol{\varepsilon}_{r_\mu}\left(\frac{1}{2}[\mathbf{y}]_\times^T+\mathbf{M}_{\mathbf{C}}^0-k_0^2\mathbf{M}_{\mathbf{C}}^1\right)\right]d\Omega_\mu =$$
$$\frac{1}{|\Omega_\mu|}\int_{\Omega_\mu}\boldsymbol{\mu}_{r_\mu}^{-1}(\mathbf{I}+\text{curl}_{\mathbf{y}}\,\mathbf{M}_{\mathbf{C}}^0)d\Omega_\mu-k_0^2\frac{1}{|\Omega_\mu|}\int_{\Omega_\mu}\left(\boldsymbol{\mu}_{r_\mu}^{-1}\,\text{curl}_{\mathbf{y}}\,\mathbf{M}_{\mathbf{C}}^1+\frac{1}{2}[\mathbf{y}]_\times\boldsymbol{\varepsilon}_{r_\mu}\left(\frac{1}{2}[\mathbf{y}]_\times^T+\mathbf{M}_{\mathbf{C}}^0\right)\right)d\Omega_\mu$$
$$+k_0^4\frac{1}{|\Omega_\mu|}\int_{\Omega_\mu}\frac{1}{2}[\mathbf{y}]_\times\boldsymbol{\varepsilon}_{r_\mu}\mathbf{M}_{\mathbf{C}}^1d\Omega_\mu =: \boldsymbol{\mu}_{\text{eff},0}^{-1}-k_0^2\boldsymbol{\mu}_{\text{eff},1}^{-1}+k_0^4\boldsymbol{\mu}_{\text{eff},2}^{-1}, \quad (4.29)$$

$$\boldsymbol{\varepsilon}_{\text{eff}} := \frac{1}{|\Omega_\mu|}\int_{\Omega_\mu}\boldsymbol{\varepsilon}_{r_\mu}d\Omega_\mu+k_0^2\frac{1}{|\Omega_\mu|}\int_{\Omega_\mu}\boldsymbol{\varepsilon}_{r_\mu}\mathbf{M}_{\mathbf{E}}^0d\Omega_\mu =: \boldsymbol{\varepsilon}_{\text{eff},0}+k_0^2\boldsymbol{\varepsilon}_{\text{eff},1}, \quad (4.30)$$

$$\boldsymbol{\chi}_{\text{eff}} := \frac{1}{|\Omega_\mu|}\int_{\Omega_\mu}\left[-\frac{1}{2}k_0^2[\mathbf{y}]_\times\boldsymbol{\varepsilon}_{r_\mu}(\mathbf{I}+k_0^2\mathbf{M}_{\mathbf{E}}^0)+k_0^2\boldsymbol{\mu}_{r_\mu}^{-1}\,\text{curl}_{\mathbf{y}}\,\mathbf{M}_{\mathbf{E}}^0\right]d\Omega_\mu =$$
$$-k_0^2\frac{1}{|\Omega_\mu|}\int_{\Omega_\mu}\left[\frac{1}{2}[\mathbf{y}]_\times\boldsymbol{\varepsilon}_{r_\mu}-\boldsymbol{\mu}_{r_\mu}^{-1}\,\text{curl}_{\mathbf{y}}\,\mathbf{M}_{\mathbf{E}}^0\right]d\Omega_\mu-k_0^4\frac{1}{|\Omega_\mu|}\int_{\Omega_\mu}\frac{1}{2}[\mathbf{y}]_\times\boldsymbol{\varepsilon}_{r_\mu}\mathbf{M}_{\mathbf{E}}^0d\Omega_\mu =:$$
$$-k_0^2\big(\boldsymbol{\chi}_{\text{eff},0}+k_0^2\boldsymbol{\chi}_{\text{eff},1}\big), \quad (4.31)$$

$$\boldsymbol{\theta}_{\text{eff}} := \frac{1}{|\Omega_\mu|}\int_{\Omega_\mu}\boldsymbol{\varepsilon}_{r_\mu}\left(\frac{1}{2}[\mathbf{y}]_\times^\top+\mathbf{M}_{\mathbf{C}}^0\right)d\Omega_\mu-k_0^2\frac{1}{|\Omega_\mu|}\int_{\Omega_\mu}\boldsymbol{\varepsilon}_{r_\mu}\mathbf{M}_{\mathbf{C}}^1d\Omega_\mu =: \boldsymbol{\theta}_{\text{eff},0}-k_0^2\boldsymbol{\theta}_{\text{eff},1}. \quad (4.32)$$

$$\boldsymbol{\mu}_{\text{eff},0}^{-1} := \frac{1}{|\Omega_\mu|}\int_{\Omega_\mu}\boldsymbol{\mu}_{r_\mu}^{-1}(\mathbf{I}+\text{curl}_{\mathbf{y}}\,\mathbf{M}_{\mathbf{C}}^0)d\Omega_\mu, \quad (4.33)$$
$$\boldsymbol{\mu}_{\text{eff},1}^{-1} := \frac{1}{|\Omega_\mu|}\int_{\Omega_\mu}\left(\boldsymbol{\mu}_{r_\mu}^{-1}\,\text{curl}_{\mathbf{y}}\,\mathbf{M}_{\mathbf{C}}^1+\frac{1}{2}[\mathbf{y}]_\times\boldsymbol{\varepsilon}_{r_\mu}\left(\frac{1}{2}[\mathbf{y}]_\times^T+\mathbf{M}_{\mathbf{C}}^0\right)\right)d\Omega_\mu, \quad (4.34)$$
$$\boldsymbol{\mu}_{\text{eff},2}^{-1} := \frac{1}{|\Omega_\mu|}\int_{\Omega_\mu}\frac{1}{2}[\mathbf{y}]_\times\boldsymbol{\varepsilon}_{r_\mu}\mathbf{M}_{\mathbf{C}}^1d\Omega_\mu, \quad (4.35)$$
$$\boldsymbol{\varepsilon}_{\text{eff},0} := \frac{1}{|\Omega_\mu|}\int_{\Omega_\mu}\boldsymbol{\varepsilon}_{r_\mu}d\Omega_\mu, \quad (4.36)$$
$$\boldsymbol{\varepsilon}_{\text{eff},1} := \frac{1}{|\Omega_\mu|}\int_{\Omega_\mu}\boldsymbol{\varepsilon}_{r_\mu}\mathbf{M}_{\mathbf{E}}^0d\Omega_\mu, \quad (4.37)$$
$$\boldsymbol{\chi}_{\text{eff},0} := \frac{1}{|\Omega_\mu|}\int_{\Omega_\mu}\left[\frac{1}{2}[\mathbf{y}]_\times\boldsymbol{\varepsilon}_{r_\mu}-\boldsymbol{\mu}_{r_\mu}^{-1}\,\text{curl}_{\mathbf{y}}\,\mathbf{M}_{\mathbf{E}}^0\right]d\Omega_\mu, \quad (4.38)$$
$$\boldsymbol{\chi}_{\text{eff},1} := \frac{1}{|\Omega_\mu|}\int_{\Omega_\mu}\frac{1}{2}[\mathbf{y}]_\times\boldsymbol{\varepsilon}_{r_\mu}\mathbf{M}_{\mathbf{E}}^0d\Omega_\mu, \quad (4.39)$$
$$\boldsymbol{\theta}_{\text{eff},0} := \frac{1}{|\Omega_\mu|}\int_{\Omega_\mu}\boldsymbol{\varepsilon}_{r_\mu}\left(\frac{1}{2}[\mathbf{y}]_\times^\top+\mathbf{M}_{\mathbf{C}}^0\right)d\Omega_\mu, \quad (4.40)$$
$$\boldsymbol{\theta}_{\text{eff},1} := \frac{1}{|\Omega_\mu|}\int_{\Omega_\mu}\boldsymbol{\varepsilon}_{r_\mu}\mathbf{M}_{\mathbf{C}}^1d\Omega_\mu. \quad (4.41)$$

Hence, variational equation (4.15) results in

$$\int_\Omega \big(\boldsymbol{\mu}^{-1}_{\text{eff},0}\,\text{curl}\,\mathbf{E}\cdot\text{curl}\,\hat{\mathbf{E}} - k_0^2\boldsymbol{\mu}^{-1}_{\text{eff},1}\,\text{curl}\,\mathbf{E}\cdot\text{curl}\,\hat{\mathbf{E}} + k_0^4\boldsymbol{\mu}^{-1}_{\text{eff},2}\,\text{curl}\,\mathbf{E}\cdot\text{curl}\,\hat{\mathbf{E}} \\ - k_0^2\boldsymbol{\varepsilon}_{\text{eff},0}\mathbf{E}\cdot\hat{\mathbf{E}} - k_0^4\boldsymbol{\varepsilon}_{\text{eff},1}\mathbf{E}\cdot\hat{\mathbf{E}} - k_0^2\boldsymbol{\chi}_{\text{eff},0}\mathbf{E}\cdot\text{curl}\,\hat{\mathbf{E}} - k_0^4\boldsymbol{\chi}_{\text{eff},1}\mathbf{E}\cdot\text{curl}\,\hat{\mathbf{E}} \\ - k_0^2\boldsymbol{\theta}_{\text{eff},0}\,\text{curl}\,\mathbf{E}\cdot\hat{\mathbf{E}} + k_0^4\boldsymbol{\theta}_{\text{eff},1}\,\text{curl}\,\mathbf{E}\cdot\hat{\mathbf{E}}\big)d\Omega = \mathcal{R}(\hat{\mathbf{E}}) \qquad \forall\hat{\mathbf{E}}\in\mathcal{V}. \quad (4.42)$$

The field equations associated to this variational equations read

$$\text{curl}\left(\boldsymbol{\mu}^{-1}_{\text{eff},0}\,\text{curl}\,\mathbf{E}\right) - k_0^2\,\text{curl}\left(\boldsymbol{\mu}^{-1}_{\text{eff},1}\,\text{curl}\,\mathbf{E}\right) + k_0^4\,\text{curl}\left(\boldsymbol{\mu}^{-1}_{\text{eff},2}\,\text{curl}\,\mathbf{E}\right) \\ - k_0^2\boldsymbol{\varepsilon}_{\text{eff},0}\mathbf{E} - k_0^4\boldsymbol{\varepsilon}_{\text{eff},1}\mathbf{E} - k_0^2\,\text{curl}\left(\boldsymbol{\chi}_{\text{eff},0}\mathbf{E}\right) - k_0^4\,\text{curl}\left(\boldsymbol{\chi}_{\text{eff},1}\mathbf{E}\right) \\ - k_0^2\boldsymbol{\theta}_{\text{eff},0}\,\text{curl}\,\mathbf{E} + k_0^4\boldsymbol{\theta}_{\text{eff},1}\,\text{curl}\,\mathbf{E} = \boldsymbol{R}, \quad (4.43)$$

where $\boldsymbol{R}$ stands for the field counter-part of the residual of (2.7). Let us further consider that the properties above do not vary along space, so

$$\boldsymbol{\mu}^{-1}_{\text{eff},0}\,\text{curl}\,\text{curl}\,\mathbf{E} - k_0^2\boldsymbol{\mu}^{-1}_{\text{eff},1}\,\text{curl}\,\text{curl}\,\mathbf{E} + k_0^4\boldsymbol{\mu}^{-1}_{\text{eff},2}\,\text{curl}\,\text{curl}\,\mathbf{E} - k_0^2\boldsymbol{\varepsilon}_{\text{eff},0}\mathbf{E} - k_0^4\boldsymbol{\varepsilon}_{\text{eff},1}\mathbf{E} \\ - k_0^2\boldsymbol{\chi}_{\text{eff},0}\,\text{curl}\,\mathbf{E} - k_0^4\boldsymbol{\chi}_{\text{eff},1}\,\text{curl}\,\mathbf{E} - k_0^2\boldsymbol{\theta}_{\text{eff},0}\,\text{curl}\,\mathbf{E} + k_0^4\boldsymbol{\theta}_{\text{eff},1}\,\text{curl}\,\mathbf{E} = \boldsymbol{R}, \quad (4.44)$$

that is

$$\boldsymbol{\mu}^{-1}_{\text{eff},0}\,\text{curl}\,\text{curl}\,\mathbf{E} - k_0^2\boldsymbol{\mu}^{-1}_{\text{eff},1}\,\text{curl}\,\text{curl}\,\mathbf{E} + k_0^4\boldsymbol{\mu}^{-1}_{\text{eff},2}\,\text{curl}\,\text{curl}\,\mathbf{E} - k_0^2\boldsymbol{\varepsilon}_{\text{eff},0}\mathbf{E} - k_0^4\boldsymbol{\varepsilon}_{\text{eff},1}\mathbf{E} \\ - k_0^2\big(\boldsymbol{\chi}_{\text{eff},0}+\boldsymbol{\theta}_{\text{eff},0}\big)\,\text{curl}\,\mathbf{E} - k_0^4\big(\boldsymbol{\chi}_{\text{eff},1}-\boldsymbol{\theta}_{\text{eff},1}\big)\,\text{curl}\,\mathbf{E} = \boldsymbol{R}. \quad (4.45)$$

Similar governing equations have been derived in the context of high-order (micromorphic) theories of electromagnetism [21]. Although this is not a full space-time high-order theory (it does not contain high-order spatial derivatives), it brings a more comprehensive picture of the microscopic electromagnetic phenomena through high-order contributions regarding time, which makes this especially interesting for high-frequency problems.

Importantly, the proposed formulation provides a systematic rational approach to derive constitutive equations that go beyond the classical characterisation of permeability and permittivity in electromagnetic media.

5. Numerical results

5.1. **Preliminaries.** In different numerical examples, we consider a cube-shaped cell with a spherical inclusion at its center. The cube-shaped block has dimensions $\ell_\mu\times\ell_\mu\times\ell_\mu$. The radius of the spherical inclusion is denoted by r_i. We define a reference wavelength λ. The wave-number is therefore given by $k_0 = 2\pi/\lambda$. In addition, we assume $\boldsymbol{\mu}_{r_\mu} = \mathbf{I}$ and $\boldsymbol{\varepsilon}_{r_\mu} = n^2\mathbf{I}$, where n is the refractive index of the medium. We also consider periodic boundary conditions to constrain the fields at the micro-cell. That is, we use the periodic space defined in (3.18). In the forthcoming numerical experiments, we will focus on the computation of the effective permittivity of the micro-cell. Hence, under the considerations presented in this section, the canonical micro-cell problems (4.22) degenerate themselves to find $\mathbf{U}^{(i)}_\mu\in\tilde{\boldsymbol{\mathcal{V}}}^P_\mu$, such that

$$\int_{\Omega_\mu}\left[\text{curl}_{\mathbf{y}}\,\mathbf{U}^{(i)}_\mu\cdot\text{curl}_{\mathbf{y}}\,\hat{\tilde{\mathbf{E}}}_\mu - k_0^2n^2\mathbf{U}^{(i)}_\mu\cdot\hat{\tilde{\mathbf{E}}}_\mu\right]d\Omega_\mu = \int_{\Omega_\mu}k_0^2n^2\mathbf{e}_i\cdot\hat{\tilde{\mathbf{E}}}_\mu d\Omega_\mu \quad \forall\hat{\tilde{\mathbf{E}}}_\mu\in\tilde{\boldsymbol{\mathcal{V}}}^P_\mu. \quad (5.1)$$

In our particular setting, n is assumed to be given by a piece-wise constant function of the form

$$n = n_1 \quad \text{in} \quad \Omega_1 \qquad \text{and} \qquad n = n_2 \quad \text{in} \quad \Omega_2, \quad (5.2)$$

with $\Omega_\mu = \Omega_1 \cup \Omega_2$, such that $\Omega_1 \cap \Omega_2 = \varnothing$. Since the cell is centro-symmetric and its constituents are isotropic, the resulting effective electric permittivity from (4.17) becomes also isotropic, which is denoted by $\varepsilon_{\text{eff}} = [\boldsymbol{\varepsilon}_{\text{eff}}]_{ii}$, with $[\boldsymbol{\varepsilon}_{\text{eff}}]_{ij} = 0$, for $i \neq j$, for $i, j = 1, 2, 3$. The volume constraint (3.12) over $\mathbf{U}_\mu^{(i)}$ is imposed via Lagrange multipliers as described in C. In addition, the variational equations are approximated via the Finite Element Method. Specifically, Nédélec finite elements are employed [28]. The implementation of this finite element approximation available in the FreeFEM++ library [23] is used in this work. Finally, once $\mathbf{U}_\mu^{(i)}$ is computed numerically for each canonical direction $\mathbf{e}_i$, the Cartesian components of the effective permittivity can be evaluated with the help of (4.17) and (4.20), namely

$$[\boldsymbol{\varepsilon}_{\text{eff}}]_{ij} = \frac{1}{|\Omega_\mu|} \int_{\Omega_\mu} n^2 \big(\delta_{ij} + [\mathbf{U}_\mu^{(j)}]_i\big) d\Omega_\mu, \tag{5.3}$$

where δ_{ij} is the Kronecker delta.

In the following numerical examples, we compare the effective dielectric permittivity of inhomogeneous media calculated with the proposed multiscale formalism to well-established analytical mixing rules to provide the necessary benchmarks for the method.

5.2. **Example 1: Long wavelength limit.** In this first example, we consider a cell of size $\ell_\mu = 1\mu$m made of glass (SiO_2) with a spherical inclusion of silicon (Si) at its center so that the refractive indexes are given by $n_1 = 2.847$ for silicon and $n_2 = 1.444$ for glass. We define a reference wavelength $\lambda = 1.55\mu$m, which implies a working frequency of 193.4THz. The wavelengths are set as $\lambda_\alpha = 2^\alpha \lambda$, with $\alpha = 1, 2, 3, 4$. The radius r_i of the spherical inclusion varies in the interval from 0.1μm to 0.45μm. In Figure 2, we present the effective permittivities for varying wavelengths with respect to the radius r_i of the spherical inclusion. In order to test the validity of the proposed model in the long wavelength limit, we compare our findings with the prediction of the Maxwell-Garnett mixing formula [33],

$$\varepsilon_{\text{eff}}^{\text{MG}} = \varepsilon_e + 3 v_f \varepsilon_e \frac{\varepsilon_i - \varepsilon_e}{\varepsilon_i + 2\varepsilon_e - v_f(\varepsilon_i - \varepsilon_e)}. \tag{5.4}$$

where v_f is the volume fraction occupied by the spherical inclusion, namely, $v_f = \frac{4}{3}\pi r_i^3$, since the size of the cell is given by $\ell_\mu = 1$. In addition, $\varepsilon_i = n_1^2$ and $\varepsilon_e = n_2^2$. From an analysis of Figure 2, we observe that the effective permittivities computed from the proposed homogenisation framework converge toward the effective permittivity predicted by the Maxwell-Garnett approximation as r_i decreases and λ_α increases, as expected.

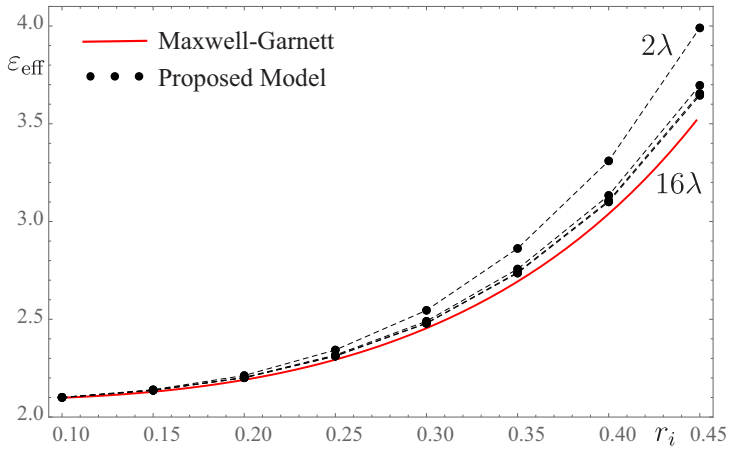

FIGURE 2. Effective permittivities for varying wavelengths $\lambda_\alpha = 2^\alpha \lambda$, with $\lambda = 1.55\mu$m and $\alpha = 1, 2, 3, 4$, with respect to the radius r_i of the spherical inclusion.

5.3. **Example 2: Resonance beyond the long wavelength limit.** In this second example, we consider again a cell of size $\ell_\mu = 1\mu$m made of glass (SiO_2) with a spherical inclusion of silicon (Si) at its center. The refractive indexes are given by $n_1 = 2.847$ and $n_2 = 1.444$ for silicon and glass, respectively. The reference wavelength is set as $\lambda = 1.55\mu$m, which induces a working frequency of 193.4THz. In order to test the validity of our model beyond the long wavelength limit, let us consider the analytical model by Wu et al. [45], which is written as

$$\varepsilon^\star_{\text{eff}} = \frac{A + BC}{1 + C}. \tag{5.5}$$

The quantities A, B and C are respectively given by

$$A = 2\varepsilon_e \frac{J_1(k_e r_e)}{J_1(k_e r_e) + k_e r_e J_1'(k_e r_e)}, \tag{5.6}$$

$$B = 2\varepsilon_e \frac{Y_1(k_e r_e)}{Y_1(k_e r_e) + k_e r_e Y_1'(k_e r_e)}, \tag{5.7}$$

$$C = \boldsymbol{i} \frac{Y_1(k_e r_e) + k_e r_e Y_1'(k_e r_e)}{J_1(k_e r_e) + k_e r_e J_1'(k_e r_e)} \left(\frac{D}{1 + D} \right), \tag{5.8}$$

where J_1 is the spherical Bessel function and Y_1 is the spherical Neumann function. In addition,

$$D = \frac{k_e \mu_i P(k_e r_i) P'(k_i r_i) - k_i \mu_e P(k_i r_i) P'(k_e r_i)}{k_i \mu_e P(k_i r_i) Q'(k_e r_i) - k_e \mu_i Q(k_e r_i) P'(k_i r_i)}, \tag{5.9}$$

where $k_i = \omega\sqrt{\varepsilon_i \mu_i}$, $k_e = \omega\sqrt{\varepsilon_e \mu_e}$, $P(x) = xJ_1(x)$ and $Q(x) = xH_1(x)$, with $H_1(x) = J_1(x) + \boldsymbol{i} Y_1(x)$. Here, $\varepsilon_i = n_1^2$, $\varepsilon_e = n_2^2$ and $\mu_i = \mu_e = 1$, as before. Finally, $r_e = \ell_\mu = 1\mu$m, and the radius of the spherical inclusion is fixed as $r_i = 0.25\mu$m.

We set $\lambda_\alpha = \alpha\lambda$, where $\lambda = 1.55\mu$m and α varies from 1 to 1.2. According to the analytical model given by (5.5), resonance occurs at $\lambda_\alpha \approx 1.69\mu$m, which is well captured by our model as shown in Figure 3, and that is absent in the Maxwell-Garnett theory. However, a small shift in the resonance frequency can be seen between both models. We have verified that the smaller the radius of the inclusion r_i, the smaller the shift in the resonance frequency. Since the wavelength is fixed, we attribute this fact to the higher-order interaction effects between inclusions, which are predicted by our model. In

contrast, the analytical model (5.5) is derived assuming that the spherical inclusion is isolated so that it does not account for interactions between the inclusions.

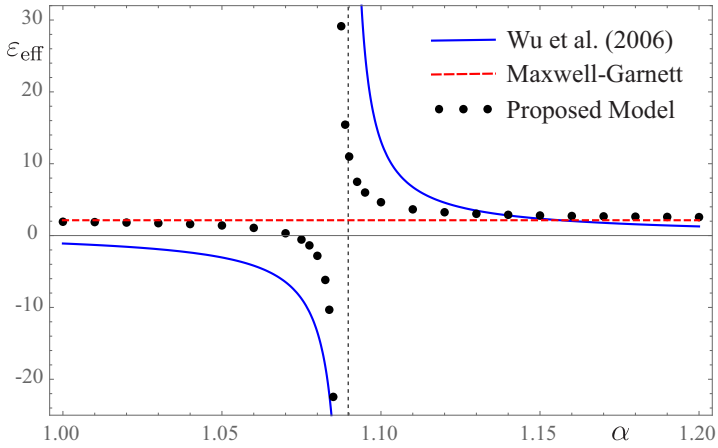

FIGURE 3. Effective permittivities for $r_i = 0.25\mu$m and varying wavelengths $\lambda_\alpha = \alpha\lambda$, with $\lambda = 1.55\mu$m and α from 1 to 1.2.

5.4. **Example 3: Phase transition.** In this last example, we test the validity of our model in the scenario where the percolation transition occurs. To accomplish this we compare our findings to the Bruggeman effective medium theory [15], one of the simplest analytical models to predict the percolation transition, in a system composed of spherical gold inclusions embedded within a polystyrene substrate. The wavelength is fixed as $\lambda = 2\mu$m, which corresponds to a working frequency of 149.9THz. According to [25], at this frequency the gold and polymer permittivities are respectively given by $\varepsilon_i = -158.08 + 19.58\boldsymbol{i}$ and $\varepsilon_e = 2.44$. The diameter of the particles is fixed as $d_i = 10$nm, while the size of the cell ℓ_μ varies from 40nm to 10nm. As said, we compare the predictions of our model to the ones delivered by the Bruggeman effective medium theory [15], and that are established by the following formula

$$\begin{aligned}(1-v_f)\left(\frac{\varepsilon_e-\varepsilon_{\text{eff}}^{\text{B}}}{\varepsilon_{\text{eff}}^{\text{B}}+L(\varepsilon_e-\varepsilon_{\text{eff}}^{\text{B}})}+\frac{4(\varepsilon_e-\varepsilon_{\text{eff}}^{\text{B}})}{2\varepsilon_{\text{eff}}^{\text{B}}+(1-L)(\varepsilon_e-\varepsilon_{\text{eff}}^{\text{B}})}\right)\\ +v_f\left(\frac{\varepsilon_i-\varepsilon_{\text{eff}}^{\text{B}}}{\varepsilon_{\text{eff}}^{\text{B}}+L(\varepsilon_i-\varepsilon_{\text{eff}}^{\text{B}})}+\frac{4(\varepsilon_i-\varepsilon_{\text{eff}}^{\text{B}})}{2\varepsilon_{\text{eff}}^{\text{B}}+(1-L)(\varepsilon_i-\varepsilon_{\text{eff}}^{\text{B}})}\right)=0,\end{aligned} \tag{5.10}$$

where $0 \leq L \leq 1$ is the depolarisation factor and the volume fraction occupied by the spherical particle $0 \leq v_f \leq 1$ is trivially computed as $v_f = \frac{\pi d_i^3}{6\ell_\mu^3}$. Therefore, once the diameter d_i of the inclusions is fixed, the smaller the size of the cell ℓ_μ, the higher the volume fraction v_f. The obtained results are reported through Figures 4 and 5, where the red cross-dot highlights the moment in which the inclusions touch each other, namely $\ell_\mu = d_i$, because of the periodicity assumption. In particular, Figures 4 and 5 display, the real and imaginary components of ε_{eff}, respectively. From the analysis of these figures it is clear that the proposed model qualitatively captures the presence of the percolation transition, which according to the Bruggeman theory is expected to occur for $f = 1/3$ in the case of spherical inclusions [15]. On the one hand, in percolative composites enhanced $\Re\{\varepsilon_{\text{eff}}\}$ occurs when the volume fraction is slightly below the percolation threshold. On the other hand, negative $\Re\{\varepsilon_{\text{eff}}\}$ is expected to occur when the volume fraction exceeds the percolation threshold. This effect has been observed experimentally in metal-dielectric composites [42]. At the same time, a large absorption within the effective medium, encoded in $\Im\{\varepsilon_{\text{eff}}\}$, occurs at the critical point, which is intrinsically related to the universal

properties of the percolation phase transition, in particular the enhanced and scale invariant current and electric field fluctuations that take place close to phase transition [31]. These effects are well captured by our model as can be seen in Figures 4 and 5.

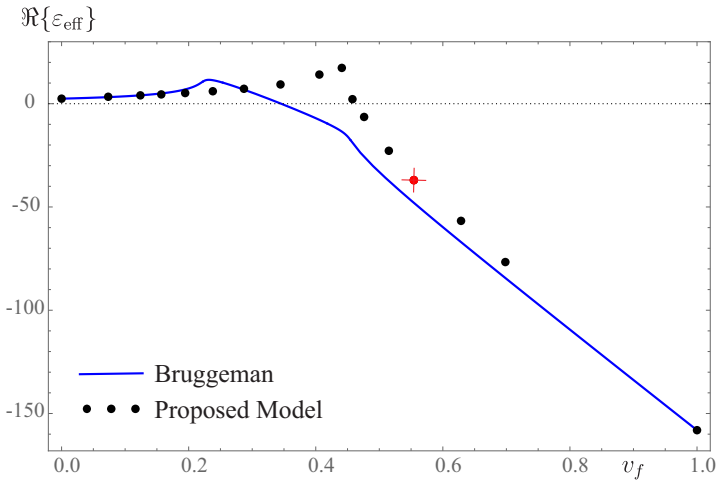

FIGURE 4. Real component of the effective permittivities ε_{eff} as a function of the volume fraction v_f occupied by the spherical inclusion of gold embedded in a host medium of polystyrene. The red cross-dot highlights the moment in which the inclusions touch each other ($\ell_\mu = d_i$).

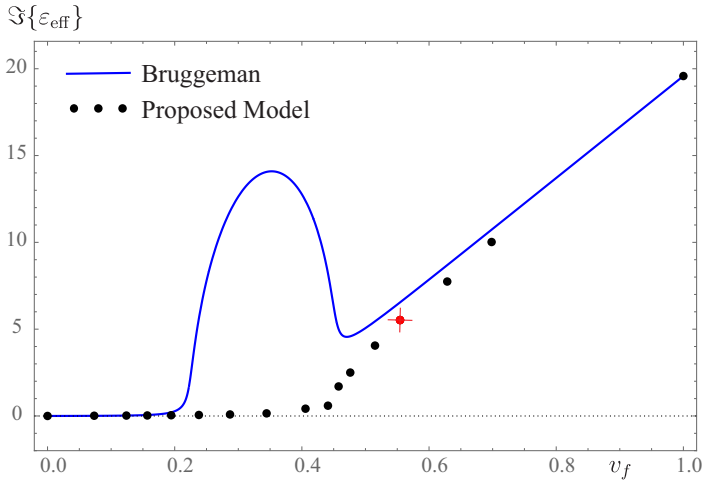

FIGURE 5. Imaginary component of the effective permittivities ε_{eff} as a function of the volume fraction v_f occupied by the spherical inclusion of gold embedded in a host medium of polystyrene. The red cross-dot highlights the moment in which the inclusions touch each other ($\ell_\mu = d_i$)

6. Concluding remarks

In this article, we have derived a novel multiscale constitutive model in which the electromagnetic macroscopic effective parameters are completely characterised by the underlying microscopic properties. In contrast to conventional homogenisation approaches, the proposed model is based on the variational framework given by the Method of Multiscale Virtual Power, which was applied here to Maxwell's equations for the first time. The resulting effective properties depend explicitly as well as implicitly on the working

frequency. The implicit dependence comes out from the solution to the micro-cell problems, which encode the complex dynamics governed by Maxwell's equations. As a result, complex macroscopic behavior has been observed through numerical experiments, including resonances and phase transitions. Indeed, we apply the method in different cases of interest ranging from low-frequency to high-frequency regimes, providing not only a physical benchmark to validate our findings but also demonstrating the predictive capabilities of the model in terms of determining effective electromagnetic properties.

Acknowledgements

This research was partly supported by CNPq (Brazilian Research Council), FAPERJ (Research Foundation of the State of Rio de Janeiro), and CAPES (Coordination for the Improvement of Higher Education Personnel). These financial supports are gratefully acknowledged. We also thank Dr. Lucas Heitzmann Gabrielli for the fruitful early discussions.

Appendix A. Vector and tensor identities

Let us introduce some vector and tensor identities that are useful in the derivations of this work.

Consider two arbitrary constant vectors $\mathbf{U}, \mathbf{V}$, then, the following identities hold

$$\mathbf{U} \cdot (\mathbf{V} \times \mathbf{y}) = (\mathbf{y} \times \mathbf{U}) \cdot \mathbf{V}, \tag{A.1}$$

$$\operatorname{curl}_{\mathbf{y}}(\mathbf{U} \times \mathbf{y}) = 2\mathbf{U}. \tag{A.2}$$

Consider arbitrary vectors $\mathbf{U}, \mathbf{V}, \mathbf{W}$. Given the cross product $\mathbf{U} \times \mathbf{V}$, let us also define the tensor $[\mathbf{U}]_\times$ as the unique skew-symmetric tensor that satisfies

$$\mathbf{U} \times \mathbf{V} = [\mathbf{U}]_\times \mathbf{V}. \tag{A.3}$$

Thus, we can write

$$\mathbf{U} \times \mathbf{V} = [\mathbf{V}]_\times^\top \mathbf{U}, \tag{A.4}$$

and we also note that

$$\operatorname{curl} \mathbf{V} \times \mathbf{U} = [\operatorname{curl} \mathbf{V}]_\times \mathbf{U} = 2(\nabla \mathbf{V})^W \mathbf{U}. \tag{A.5}$$

As well, let us recall that

$$\mathbf{U} \times (\mathbf{V} \times \mathbf{W}) = (\mathbf{U} \cdot \mathbf{W})\mathbf{V} - (\mathbf{U} \cdot \mathbf{V})\mathbf{W}. \tag{A.6}$$

Particularly, consider $\mathbf{y}$ the micro-scale coordinate vector. In a Cartesian coordinate system, it is $\mathbf{y} = (y_1, y_2, y_3)^\top$, with $y_i = \mathbf{y} \cdot \mathbf{e}_i$. Therefore, tensor $[\mathbf{y}]_\times$ reads

$$[\mathbf{y}]_\times = \begin{pmatrix} 0 & -y_3 & y_2 \\ y_3 & 0 & -y_1 \\ -y_2 & y_1 & 0 \end{pmatrix}. \tag{A.7}$$

In addition, $[\mathbf{y}]_\times^\top = -[\mathbf{y}]_\times$.

The curl of a second order tensor $\mathbf{L}$ is defined as the second order tensor $\operatorname{curl} \mathbf{L}$ that, for any constant vector $\mathbf{V}$, satisfies the following

$$(\operatorname{curl} \mathbf{L})\mathbf{V} = \operatorname{curl}(\mathbf{L}\mathbf{V}). \tag{A.8}$$

Observe that in Cartesian coordinates it is

$$\operatorname{curl} \mathbf{L} = [\boldsymbol{\epsilon}]_{imn} \frac{\partial [\mathbf{L}]_{nj}}{\partial x_m} (\mathbf{e}_i \otimes \mathbf{e}_j), \tag{A.9}$$

where $\boldsymbol{\epsilon}$ is the Levi-Civita third-order tensor, whose components in three spatial dimensions are defined as follows

$$[\boldsymbol{\epsilon}]_{ijk} = \begin{cases} 1 & \text{if } (i,j,k) \text{ is an even permutation of } (1,2,3), \\ -1 & \text{if } (i,j,k) \text{ is an odd permutation of } (1,2,3), \\ 0 & \text{if } i=j \text{ or } j=k \text{ or } i=k. \end{cases} \tag{A.10}$$

Appendix B. Derivation of tangent operators

The first step to characterize the tangent relations between the homogenised dual entities $(\mathbf{D}_{|\mathbf{x}}, \mathbf{H}_{|\mathbf{x}})$ and the primal variables $(\mathbf{E}_{|\mathbf{x}}, \mathbf{C}_{|\mathbf{x}})$ consists in deriving the variational problem (4.11) to characterize the tangent relation between $\tilde{\mathbf{E}}_\mu$ and the pair $(\mathbf{E}_{|\mathbf{x}}, \mathbf{C}_{|\mathbf{x}})$. This implies establishing the expression of the Gâteaux derivative of operator $\mathcal{M}_\mu$ from (4.12), with respect to the pair $(\mathbf{E}_{|\mathbf{x}}, \mathbf{C}_{|\mathbf{x}})$.

Consider problem (4.11), but instead of $\mathbf{E}_{|\mathbf{x}}$ we put $\mathbf{E}_{|\mathbf{x}} + \tau\delta\mathbf{E}_{|\mathbf{x}}$. This perturbation will yield a perturbation in the fluctuation field of the form $\tilde{\mathbf{E}}_\mu + \tau\delta_{\mathbf{E}}\tilde{\mathbf{E}}_\mu$. After taking the derivative with respect to τ, and making $\tau = 0$, the linear problem reads

$$\int_{\Omega_\mu} \big(\boldsymbol{\mu}_{r_\mu}^{-1} \operatorname{curl}_{\mathbf{y}} \delta_{\mathbf{E}}\tilde{\mathbf{E}}_\mu \cdot \operatorname{curl}_{\mathbf{y}} \hat{\tilde{\mathbf{E}}}_\mu - k_0^2 \boldsymbol{\varepsilon}_{r_\mu}\big(\delta\mathbf{E}_{|\mathbf{x}} + \delta_{\mathbf{E}}\tilde{\mathbf{E}}_\mu\big) \cdot \hat{\tilde{\mathbf{E}}}_\mu\big) d\Omega_\mu = 0 \qquad \forall \hat{\tilde{\mathbf{E}}}_\mu \in \tilde{\boldsymbol{\mathcal{V}}}_\mu. \tag{B.1}$$

For a given $\delta\mathbf{E}_{|\mathbf{x}}$, this variational equation amounts to find $\delta_{\mathbf{E}}\tilde{\mathbf{E}}_\mu \in \tilde{\boldsymbol{\mathcal{V}}}_\mu$ such that

$$\int_{\Omega_\mu} \big(\boldsymbol{\mu}_{r_\mu}^{-1} \operatorname{curl}_{\mathbf{y}} \delta_{\mathbf{E}}\tilde{\mathbf{E}}_\mu \cdot \operatorname{curl}_{\mathbf{y}} \hat{\tilde{\mathbf{E}}}_\mu - k_0^2 \boldsymbol{\varepsilon}_{r_\mu} \delta_{\mathbf{E}}\tilde{\mathbf{E}}_\mu \cdot \hat{\tilde{\mathbf{E}}}_\mu\big) d\Omega_\mu = \int_{\Omega_\mu} k_0^2 \boldsymbol{\varepsilon}_{r_\mu} \delta\mathbf{E}_{|\mathbf{x}} \cdot \hat{\tilde{\mathbf{E}}}_\mu d\Omega_\mu \qquad \forall \hat{\tilde{\mathbf{E}}}_\mu \in \tilde{\boldsymbol{\mathcal{V}}}_\mu. \tag{B.2}$$

Expression (B.2) defines the following tangent operator

$$\begin{aligned} \delta_{\mathbf{E}}\tilde{\mathbf{E}}_\mu &= \delta\mathcal{M}_\mu((\mathbf{E}_{|\mathbf{x}}, \mathbf{C}_{|\mathbf{x}}), (\delta\mathbf{E}_{|\mathbf{x}}, \mathbf{0})) \\ &= \frac{d}{d\tau}\mathcal{M}_\mu(\mathbf{E}_{|\mathbf{x}} + \tau\delta\mathbf{E}_{|\mathbf{x}}, \mathbf{C}_{|\mathbf{x}})\Big|_{\tau=0} \\ &= \mathbf{M}_{\mathbf{E}}\delta\mathbf{E}_{|\mathbf{x}}. \end{aligned} \tag{B.3}$$

Since the variational problem (B.2) is uncoupled and linear, we can write $\delta_{\mathbf{E}}\tilde{\mathbf{E}}_\mu$ in terms of the Cartesian components of $\delta\mathbf{E}_{|\mathbf{x}}$ as $\delta_{\mathbf{E}}\tilde{\mathbf{E}}_\mu = [\delta\mathbf{E}_{|\mathbf{x}}]_i\, \mathbf{U}_\mu^{(i)}$, where $[\delta\mathbf{E}_{|\mathbf{x}}]_i = \delta\mathbf{E}_{|\mathbf{x}} \cdot \mathbf{e}_i$ and $\mathbf{U}_\mu^{(i)} \in \tilde{\boldsymbol{\mathcal{V}}}_\mu$, for $i = 1,2,3$, solve the set of canonical variational problems (4.22). In addition, we have $\delta_{\mathbf{E}}\tilde{\mathbf{E}}_\mu = (\delta\mathbf{E}_{|\mathbf{x}} \cdot \mathbf{e}_j)[\mathbf{U}_\mu^{(j)}]_i\, \mathbf{e}_i = [\mathbf{U}_\mu^{(j)}]_i\, (\mathbf{e}_i \otimes \mathbf{e}_j)\delta\mathbf{E}_{|\mathbf{x}}$, with $[\mathbf{U}_\mu^{(j)}]_i = \mathbf{U}_\mu^{(j)} \cdot \mathbf{e}_i$. From these elements, the tangent operator (B.3) can be characterised by

$$\mathbf{M}_{\mathbf{E}} = [\mathbf{U}_\mu^{(j)}]_i\, (\mathbf{e}_i \otimes \mathbf{e}_j). \tag{B.4}$$

Similarly, consider the same problem (4.11), but now instead of $\mathbf{C}_{|\mathbf{x}}$ we insert $\mathbf{C}_{|\mathbf{x}} + \tau\delta\mathbf{C}_{|\mathbf{x}}$. Such a perturbation will result in a modification of the fluctuation field of the form $\tilde{\mathbf{E}}_\mu + \tau\delta_{\mathbf{C}}\tilde{\mathbf{E}}_\mu$. After taking the derivative with respect to τ, and making $\tau = 0$, the corresponding linear problem is

$$\int_{\Omega_\mu} \Big[\boldsymbol{\mu}_{r_\mu}^{-1}\big(\delta\mathbf{C}_{|\mathbf{x}} + \operatorname{curl}_{\mathbf{y}} \delta_{\mathbf{C}}\tilde{\mathbf{E}}_\mu\big) \cdot \operatorname{curl}_{\mathbf{y}} \hat{\tilde{\mathbf{E}}}_\mu - k_0^2 \boldsymbol{\varepsilon}_{r_\mu}\Big(\frac{1}{2}\delta\mathbf{C}_{|\mathbf{x}} \times \mathbf{y} + \delta_{\mathbf{C}}\tilde{\mathbf{E}}_\mu\Big) \cdot \hat{\tilde{\mathbf{E}}}_\mu\Big] d\Omega_\mu = 0 \qquad \forall \hat{\tilde{\mathbf{E}}}_\mu \in \tilde{\boldsymbol{\mathcal{V}}}_\mu. \tag{B.5}$$

Therefore, given $\delta\mathbf{C}_{|\mathbf{x}}$, the above variational equation implies finding $\delta_{\mathbf{C}}\tilde{\mathbf{E}}_\mu \in \tilde{\boldsymbol{\mathcal{V}}}_\mu$ such that

$$\int_{\Omega_\mu} \big(\boldsymbol{\mu}_{r_\mu}^{-1}\,\mathrm{curl}_{\mathbf{y}}\,\delta_{\mathbf{C}}\tilde{\mathbf{E}}_\mu \cdot \mathrm{curl}_{\mathbf{y}}\,\hat{\tilde{\mathbf{E}}}_\mu - k_0^2\boldsymbol{\varepsilon}_{r_\mu}\delta_{\mathbf{C}}\tilde{\mathbf{E}}_\mu \cdot \hat{\tilde{\mathbf{E}}}_\mu\big)d\Omega_\mu = \int_{\Omega_\mu}\Big[-\boldsymbol{\mu}_{r_\mu}^{-1}\delta\mathbf{C}_{|\mathbf{x}} \cdot \mathrm{curl}_{\mathbf{y}}\,\hat{\tilde{\mathbf{E}}}_\mu + \frac{1}{2}k_0^2\boldsymbol{\varepsilon}_{r_\mu}(\delta\mathbf{C}_{|\mathbf{x}}\times\mathbf{y})\cdot\hat{\tilde{\mathbf{E}}}_\mu\Big]d\Omega_\mu \qquad \forall\hat{\tilde{\mathbf{E}}}_\mu \in \tilde{\boldsymbol{\mathcal{V}}}_\mu. \quad \text{(B.6)}$$

In this case, expression (B.6) defines the following tangent operator

$$\begin{aligned}\delta_{\mathbf{C}}\tilde{\mathbf{E}}_\mu &= \delta\mathcal{M}_\mu((\mathbf{E}_{|\mathbf{x}},\mathbf{C}_{|\mathbf{x}}),(\mathbf{0},\delta\mathbf{C}_{|\mathbf{x}}))\\ &= \frac{d}{d\tau}\mathcal{M}_\mu(\mathbf{E}_{|\mathbf{x}},\mathbf{C}_{|\mathbf{x}}+\tau\delta\mathbf{C}_{|\mathbf{x}})\Big|_{\tau=0}\\ &= \mathbf{M}_{\mathbf{C}}\delta\mathbf{C}_{|\mathbf{x}}.\end{aligned} \quad \text{(B.7)}$$

Following the same steps as before, we define $\delta_{\mathbf{C}}\tilde{\mathbf{E}}_\mu = [\delta\mathbf{C}_{|\mathbf{x}}]_i\,\mathbf{V}_\mu^{(i)}$, where $\mathbf{V}_\mu^{(i)} \in \tilde{\boldsymbol{\mathcal{V}}}_\mu$, for $i=1,2,3$, solve the set of canonical variational problems (4.23). Therefore, the tangent operator from (B.7) can be characterised by

$$\mathbf{M}_{\mathbf{C}} = [\mathbf{V}_\mu^{(j)}]_i\,(\mathbf{e}_i\otimes\mathbf{e}_j). \quad \text{(B.8)}$$

Now, we can write (4.7) as follows

$$\begin{aligned}\mathbf{D}_{|\mathbf{x}}(\mathbf{E}_{|\mathbf{x}},\mathbf{C}_{|\mathbf{x}}) = &\left(\frac{1}{|\Omega_\mu|}\int_{\Omega_\mu}\boldsymbol{\varepsilon}_{r_\mu}d\Omega_\mu\right)\mathbf{E}_{|\mathbf{x}}\\ &+\frac{1}{2}\left(\frac{1}{|\Omega_\mu|}\int_{\Omega_\mu}\boldsymbol{\varepsilon}_{r_\mu}[\mathbf{y}]_\times^\top\right)\mathbf{C}_{|\mathbf{x}}\\ &+\frac{1}{|\Omega_\mu|}\int_{\Omega_\mu}\boldsymbol{\varepsilon}_{r_\mu}\tilde{\mathbf{E}}_\mu(\mathbf{E}_{|\mathbf{x}},\mathbf{C}_{|\mathbf{x}})d\Omega_\mu.\end{aligned} \quad \text{(B.9)}$$

The last term above brings additional high-order terms to the homogenisation of the displacement field $\mathbf{D}$. The expression (B.9) above is the multiscale version of (2.8). In fact, using (B.3) and (B.7), we can write now the following tangent relation

$$\frac{d}{d\tau}\mathbf{D}_{|\mathbf{x}}(\mathbf{E}_{|\mathbf{x}}+\tau\delta\mathbf{E}_{|\mathbf{x}},\mathbf{C}_{|\mathbf{x}}+\tau\delta\mathbf{C}_{|\mathbf{x}})\Big|_{\tau=0} = (\mathcal{D}_{\mathbf{E}}\mathbf{D}_{|\mathbf{x}})\delta\mathbf{E}_{|\mathbf{x}} + (\mathcal{D}_{\mathbf{C}}\mathbf{D}_{|\mathbf{x}})\delta\mathbf{C}_{|\mathbf{x}}. \quad \text{(B.10)}$$

where $\mathcal{D}_{\mathbf{E}}\mathbf{D}_{|\mathbf{x}}$ and $\mathcal{D}_{\mathbf{C}}\mathbf{D}_{|\mathbf{x}}$ are second-order tensors defined as

$$\mathcal{D}_{\mathbf{E}}\mathbf{D}_{|\mathbf{x}} = \frac{1}{|\Omega_\mu|}\int_{\Omega_\mu}\boldsymbol{\varepsilon}_{r_\mu}(\mathbf{I}+\mathbf{M}_{\mathbf{E}})d\Omega_\mu, \quad \text{(B.11)}$$

$$\mathcal{D}_{\mathbf{C}}\mathbf{D}_{|\mathbf{x}} = \frac{1}{|\Omega_\mu|}\int_{\Omega_\mu}\boldsymbol{\varepsilon}_{r_\mu}\left(\frac{1}{2}[\mathbf{y}]_\times^\top + \mathbf{M}_{\mathbf{C}}\right)d\Omega_\mu. \quad \text{(B.12)}$$

From the definitions (4.14), the effective electric relative permittivity is

$$\boldsymbol{\varepsilon}_{\text{eff}} := \frac{1}{|\Omega_\mu|}\int_{\Omega_\mu}\boldsymbol{\varepsilon}_{r_\mu}\big(\mathbf{I}+\mathbf{M}_{\mathbf{E}}\big)d\Omega_\mu. \quad \text{(B.13)}$$

Analogously, we can write (4.10) as follows

$$\begin{aligned}\mathbf{H}_{|\mathbf{x}}(\mathbf{E}_{|\mathbf{x}},\mathbf{C}_{|\mathbf{x}}) = &\left(\frac{1}{|\Omega_\mu|}\int_{\Omega_\mu}\boldsymbol{\mu}_{r_\mu}^{-1}d\Omega_\mu\right)\mathbf{C}_{|\mathbf{x}}\\ &+\frac{1}{|\Omega_\mu|}\int_{\Omega_\mu}\boldsymbol{\mu}_{r_\mu}^{-1}\,\mathrm{curl}_{\mathbf{y}}\,\tilde{\mathbf{E}}_\mu(\mathbf{E}_{|\mathbf{x}},\mathbf{C}_{|\mathbf{x}})d\Omega_\mu\\ &-\frac{1}{2}k_0^2\left(\frac{1}{|\Omega_\mu|}\int_{\Omega_\mu}[\mathbf{y}]_\times\boldsymbol{\varepsilon}_{r_\mu}d\Omega_\mu\right)\mathbf{E}_{|\mathbf{x}}\\ &-\frac{1}{4}k_0^2\left(\frac{1}{|\Omega_\mu|}\int_{\Omega_\mu}[\mathbf{y}]_\times\boldsymbol{\varepsilon}_{r_\mu}[\mathbf{y}]_\times^T d\Omega_\mu\right)\mathbf{C}_{|\mathbf{x}}\\ &-\frac{1}{2}k_0^2\frac{1}{|\Omega_\mu|}\int_{\Omega_\mu}[\mathbf{y}]_\times\boldsymbol{\varepsilon}_{r_\mu}\tilde{\mathbf{E}}_\mu(\mathbf{E}_{|\mathbf{x}},\mathbf{C}_{|\mathbf{x}})d\Omega_\mu. \end{aligned}\tag{B.14}$$

Rearranging terms, results

$$\begin{aligned}\mathbf{H}_{|\mathbf{x}}(\mathbf{E}_{|\mathbf{x}},\mathbf{C}_{|\mathbf{x}}) = &\left(\frac{1}{|\Omega_\mu|}\int_{\Omega_\mu}\left[\boldsymbol{\mu}_{r_\mu}^{-1}-\frac{1}{4}k_0^2[\mathbf{y}]_\times\boldsymbol{\varepsilon}_{r_\mu}[\mathbf{y}]_\times^T\right]d\Omega_\mu\right)\mathbf{C}_{|\mathbf{x}}\\ &-\frac{1}{2}k_0^2\left(\frac{1}{|\Omega_\mu|}\int_{\Omega_\mu}[\mathbf{y}]_\times\boldsymbol{\varepsilon}_{r_\mu}d\Omega_\mu\right)\mathbf{E}_{|\mathbf{x}}\\ &+\frac{1}{|\Omega_\mu|}\int_{\Omega_\mu}\left[\boldsymbol{\mu}_{r_\mu}^{-1}\,\mathrm{curl}_{\mathbf{y}}\,\tilde{\mathbf{E}}_\mu(\mathbf{E}_{|\mathbf{x}},\mathbf{C}_{|\mathbf{x}})-\frac{1}{2}k_0^2[\mathbf{y}]_\times\boldsymbol{\varepsilon}_{r_\mu}\tilde{\mathbf{E}}_\mu(\mathbf{E}_{|\mathbf{x}},\mathbf{C}_{|\mathbf{x}})\right]d\Omega_\mu. \end{aligned}\tag{B.15}$$

As before, the last term in the previous expression accounts for the effect of high-order terms in the homogenisation of the magnetizing field $\mathbf{H}$. The previous expression (B.15) is the multiscale version of (2.9). Hence, from (B.3) and (B.7) we can write now the following tangent relation

$$\frac{d}{d\tau}\mathbf{H}_{|\mathbf{x}}(\mathbf{E}_{|\mathbf{x}}+\tau\delta\mathbf{E}_{|\mathbf{x}},\mathbf{C}_{|\mathbf{x}}+\tau\delta\mathbf{C}_{|\mathbf{x}})\Big|_{\tau=0} = (\mathcal{D}_{\mathbf{E}}\mathbf{H}_{|\mathbf{x}})\mathbf{E}_{|\mathbf{x}}+(\mathcal{D}_{\mathbf{C}}\mathbf{H}_{|\mathbf{x}})\mathbf{C}_{|\mathbf{x}}.\tag{B.16}$$

where $\mathcal{D}_{\mathbf{E}}\mathbf{H}_{|\mathbf{x}}$ and $\mathcal{D}_{\mathbf{C}}\mathbf{H}_{|\mathbf{x}}$ are second-order tensors defined as

$$\mathcal{D}_{\mathbf{E}}\mathbf{H}_{|\mathbf{x}} = \frac{1}{|\Omega_\mu|}\int_{\Omega_\mu}\left[-\frac{1}{2}k_0^2[\mathbf{y}]_\times\boldsymbol{\varepsilon}_{r_\mu}(\mathbf{I}+\mathbf{M}_{\mathbf{E}})+\boldsymbol{\mu}_{r_\mu}^{-1}\,\mathrm{curl}_{\mathbf{y}}\,\mathbf{M}_{\mathbf{E}}\right]d\Omega_\mu,\tag{B.17}$$

$$\mathcal{D}_{\mathbf{C}}\mathbf{H}_{|\mathbf{x}} = \frac{1}{|\Omega_\mu|}\int_{\Omega_\mu}\left[\boldsymbol{\mu}_{r_\mu}^{-1}(\mathbf{I}+\mathrm{curl}_{\mathbf{y}}\,\mathbf{M}_{\mathbf{C}})-\frac{1}{2}k_0^2[\mathbf{y}]_\times\boldsymbol{\varepsilon}_{r_\mu}\left(\frac{1}{2}[\mathbf{y}]_\times^T+\mathbf{M}_{\mathbf{C}}\right)\right]d\Omega_\mu.\tag{B.18}$$

Hence, the inverse of the effective magnetic relative permeability is defined as

$$\boldsymbol{\mu}_{\mathrm{eff}}^{-1} := \frac{1}{|\Omega_\mu|}\int_{\Omega_\mu}\left[\boldsymbol{\mu}_{r_\mu}^{-1}(\mathbf{I}+\mathrm{curl}_{\mathbf{y}}\,\mathbf{M}_{\mathbf{C}})-\frac{1}{2}k_0^2[\mathbf{y}]_\times\boldsymbol{\varepsilon}_{r_\mu}\left(\frac{1}{2}[\mathbf{y}]_\times^T+\mathbf{M}_{\mathbf{C}}\right)\right]d\Omega_\mu.\tag{B.19}$$

Appendix C. On the imposition of the volume constraint

Here we describe the method for imposing the volume constraint (3.12). The characterisation of the tangent operators (B.3) and (B.7) requires the solution of problems (4.22) and (4.23), respectively. According to the assumption of periodic micro-structured material, these problems have to be solved in the space $\boldsymbol{\mathcal{V}}_\mu^P$ defined in (3.18).

At the algebraic level, after a proper approximation of the functional spaces was introduced, say $\tilde{\mathbf{V}}^P \subset \boldsymbol{\mathcal{V}}_\mu^P$, these problems amount to solve a system of linear equations of the form

$$\mathbf{A}\tilde{\mathbf{E}}\cdot\hat{\mathbf{E}} = \mathbf{f}\cdot\hat{\mathbf{E}} \qquad \forall\hat{\mathbf{E}}\in\tilde{\mathbf{V}}^P,\tag{C.1}$$

where $\tilde{\mathbf{V}}^P$ is the finite-dimensional space in which the approximate solution is sought, noting that it contains a boundary constraint related to the periodic assumption, and the volume constraint (3.12).

Also, (C.1) can be interpreted as follows

$$\mathbf{A}\tilde{\mathbf{E}} - \mathbf{f} \perp \tilde{\mathbf{V}}^P. \tag{C.2}$$

In practice, the prescription of periodic boundary conditions is relatively straightforward and does not present challenges for the computational implementation.

In turn, volume constraint (3.12) involves coupling all the degrees of freedom in the expansion of the approximate solution. One approach to address this problem is to write an augmented system where the constraint has been removed from the space $\tilde{\mathbf{V}}^P$ using a Lagrange multiplier, say $\boldsymbol{\lambda} \in \mathbb{C}^3$. Hence, the augmented algebraic system reads as follows

$$\begin{pmatrix} \mathbf{A}_p & \mathbf{B} \\ \mathbf{B}^T & \mathbf{O} \end{pmatrix} \begin{pmatrix} \tilde{\mathbf{E}}_p \\ \boldsymbol{\lambda}_p \end{pmatrix} = \begin{pmatrix} \mathbf{f}_p \\ \mathbf{0} \end{pmatrix}, \tag{C.3}$$

where $\mathbf{O} \in \mathbb{C}^{3\times 3}$ is the null matrix, $\mathbf{0} \in \mathbb{C}^3$ is the null vector, block matrix $\mathbf{B} \in \mathbb{C}^{3m\times 3}$ stands for the discrete counterpart of the average operator, and $\mathbf{B}^T \in \mathbb{C}^{3\times 3m}$ its transpose, being m the number of independent nodes in the finite element mesh (after removing the nodes with the periodic boundary condition). Index p indicates that the operator $\mathbf{A}_p \in \mathbb{C}^{3m\times 3m}$ and vector $\mathbf{f}_p \in \mathbb{C}^{3m}$ have been reduced consistently with the periodic boundary condition, and therefore, the solution $(\tilde{\mathbf{E}}_p, \boldsymbol{\lambda}_p) \in \mathbb{C}^{3m} \times \mathbb{C}^3$ corresponds to that particular choice of boundary conditions.

Manipulating the first equation from (C.3), we get

$$\mathbf{A}_p\tilde{\mathbf{E}}_p = \mathbf{f}_p - \mathbf{B}\boldsymbol{\lambda}_p, \tag{C.4}$$

then, using the second equation from (C.3), we obtain

$$\mathbf{B}^T\tilde{\mathbf{E}}_p = \mathbf{B}^T\mathbf{A}_p^{-1}(\mathbf{f}_p - \mathbf{B}\boldsymbol{\lambda}_p) = \mathbf{0}. \tag{C.5}$$

The explicit form of the Lagrange multiplier results from solving the following system of three equations and three unknowns

$$[\mathbf{B}^T\mathbf{A}_p^{-1}\mathbf{B}]\boldsymbol{\lambda}_p = \mathbf{B}^T\mathbf{A}_p^{-1}\mathbf{f}_p. \tag{C.6}$$

That is

$$\boldsymbol{\lambda}_p = [\mathbf{B}^T\mathbf{A}_p^{-1}\mathbf{B}]^{-1}\mathbf{B}^T\mathbf{A}_p^{-1}\mathbf{f}_p. \tag{C.7}$$

Replacing (C.7) into (C.4) yields

$$\mathbf{A}_p\tilde{\mathbf{E}}_p = \mathbf{f}_p - \mathbf{B}[\mathbf{B}^T\mathbf{A}_p^{-1}\mathbf{B}]^{-1}\mathbf{B}^T\mathbf{A}_p^{-1}\mathbf{f}_p, \tag{C.8}$$

Importantly, it is not necessary to compute the explicit form of $\mathbf{A}_p^{-1}$. Instead, we have to solve the following auxiliary problems

$$\mathbf{A}_p\mathbf{y} = \mathbf{f}_p, \tag{C.9}$$

$$\mathbf{A}_p\mathbf{Z} = \mathbf{B}, \tag{C.10}$$

where $\mathbf{y} \in \mathbb{C}^{3m}$, and $\mathbf{Z} \in \mathbb{C}^{3m\times 3}$. Hence, (C.7) results

$$\boldsymbol{\lambda}_p = [\mathbf{B}^T\mathbf{Z}]^{-1}\mathbf{B}^T\mathbf{y}, \tag{C.11}$$

and (C.8) becomes

$$\mathbf{A}_p\tilde{\mathbf{E}}_p = \mathbf{f}_p - \mathbf{B}[\mathbf{B}^T\mathbf{Z}]^{-1}\mathbf{B}^T\mathbf{y}. \tag{C.12}$$

Note that matrix $\mathbf{B}^T\mathbf{Z} \in \mathbb{C}^{3\times 3}$ is not expensive to invert. In turn, problem (C.9) and each one of the 3 problems (C.10) have the same cost as the original problem, all with size $3m$.

References

[1] Omar A. M. Abdelraouf, Ziyu Wang, Hailong Liu, Zhaogang Dong, Qian Wang, Ming Ye, Xiao Renshaw Wang, Qi Jie Wang, and Hong Liu. Recent advances in tunable metasurfaces: Materials, design, and applications. *ACS Nano*, 16(9):13339–13369, 2022.

[2] Abiti Adili, Yue Chen, Robert Lipton, and Shawn Walker. Controlling the dispersion of metamaterials in three dimensions. *Proceedings of the Royal Society A: Mathematical, Physical and Engineering Sciences*, 478(2263):20220194, 2022.

[3] Grégoire Allaire. Homogenization and two-scale convergence. *SIAM J. Math. Anal.*, 23(6):1482–1518, 1992.

[4] Grégoire Allaire and Carlos Conca. Bloch-wave homogenization for a spectral problem in fluid-solid structures. *Archive for Rational Mechanics and Analysis*, 135(3):197–257, 1996.

[5] Youcef Amirat and Vladimir Shelukhin. Homogenization of time harmonic maxwell equations and the frequency dispersion effect. *Journal des Mathematiques Pures et Appliquees*, 95(4):420–443, 2011.

[6] Alireza V. Amirkhizi and Sia Nemat-Nasser. Microstructurally-based homogenization of electromagnetic properties of periodic media. *Comptes Rendus - Mecanique*, 336(1-2):24–33, 2008.

[7] H.T. Banks, V.A. Bokil, D. Cioranescu, N.L. Gibson, G. Griso, and B. Miara. Homogenization of periodically varying coefficients in electromagnetic materials. *Journal of Scientific Computing*, 28(2-3):191–221, 2006.

[8] Pablo J. Blanco and Sebastián M. Giusti. Thermomechanical multiscale constitutive modeling: Accounting for microstructural thermal effects. *Journal of Elasticity*, 115(1):27–46, 2014.

[9] Pablo J. Blanco, Pablo J. Sánchez, Eduardo A. de Souza Neto, and Raúl A. Feijóo. Variational foundations and generalized unified theory of RVE-based multiscale models. *Archives of Computational Methods in Engineering*, 23(2):191–253, 2016.

[10] P.J. Blanco, A. Clausse, and R.A. Feijóo. Homogenization of the navier-stokes equations by means of the multi-scale virtual power principle. *Computer Methods in Applied Mechanics and Engineering*, 315:760–779, 2017.

[11] P.J. Blanco, P.J. Sánchez, E.A. De Souza Neto, and R.A. Feijóo. The method of multiscale virtual power for the derivation of a second order mechanical model. *Mechanics of Materials*, 99:53–67, 2016.

[12] P.J. Blanco, P.J. Sánchez, F.F. Rocha, S. Toro, and R.A. Feijóo. A consistent multiscale mechanical formulation for media with randomly distributed voids. *International Journal of Solids and Structures*, 283:112494, 2023.

[13] Guy Bouchitté, Sébastien Guenneau, and Frédéric Zolla. Homogenization of dielectric photonic quasi crystals. *Multiscale Modeling and Simulation*, 8(5):1862–1881, 2010.

[14] Guy Bouchitté and Ben Schweizer. Homogenization of Maxwell's equations in a split ring geometry. *Multiscale Modeling and Simulation*, 8(3):717–750, 2010.

[15] F. Brouers. Percolation threshold and conductivity in metal-insulator composite mean-field theories. *Journal of Physics C: Solid State Physics*, 19(36):7183, 1986.

[16] Hou-Tong Chen, Willie J. Padilla, Joshua M. O. Zide, Arthur C. Gossard, Antoinette J. Taylor, and Richard D. Averitt. Active terahertz metamaterial devices. *Nature*, 444(7119):597–600, 2006.

[17] Kirill D. Cherednichenko and James A. Evans. Full two-scale asymptotic expansion and higher-order constitutive laws in the homogenization of the system of quasi-static maxwell equations. *Multiscale Modeling and Simulation*, 14(4):1513–1539, 2016.

[18] R.V. Craster, J. Kaplunov, E. Nolde, and S. Guenneau. Bloch dispersion and high frequency homogenization for separable doubly-periodic structures. *Wave Motion*, 49(2):333–346, 2012.

[19] E.A. De Souza Neto, P.J. Blanco, P.J. Sánchez, and R.A. Feijóo. An RVE-based multiscale theory of solids with micro-scale inertia and body force effects. *Mechanics of Materials*, 80(Part A):136–144, 2015.

[20] Christopher A. Dirdal, Hans Olaf Hagenvik, Haakon Aamot Haave, and Johannes Skaar. Higher order multipoles in metamaterial homogenization. *IEEE Transactions on Antennas and Propagation*, 66(11):6403–6407, 2018.

[21] A. Cemal Eringen. Micromorphic electromagnetic theory and waves. *Foundations of Physics*, 36(6):902–919, 2006.

[22] A.C. Eringen and G.A. Maugin. *Electrodynamics of continua I: Foundations and Solid Media*. Springer-Verlag, 1990.

[23] Frédéric Hecht. FreeFEM documentation. Release 4.13. 2022. https://doc.freefem.org/introduction/index.html.

[24] Saman Jahani and Zubin Jacob. All-dielectric metamaterials. *Nature Nanotechnology*, 11(1):23–36, 2016.

[25] P.B. Johnson and R.W. Christy. Optical constants of the noble metals. *Physical Review B*, 6(12):4370, 1972.

[26] Yongmin Liu and Xiang Zhang. Metamaterials: A new frontier of science and technology. *Chemical Society Reviews*, 40(5):2494–2507, 2011.

[27] B. Maling, D.J. Colquitt, and R.V. Craster. Dynamic homogenisation of maxwell's equations with applications to photonic crystals and localised waveforms on gratings. *Wave Motion*, 69:35–49, 2017.

[28] J.C. Nédélec. Mixed finite elements in $\mathbb{R}^3$. *Numerische Mathematik*, 35:315–341, 1980.

[29] Gabriel Nguetseng. A general convergence result for a functional related to the theory of homogenization. *SIAM J. Math. Anal.*, 20(3):608–623, 1989.

[30] Felipe Figueredo Rocha, Pablo Javier Blanco, Pablo Javier Sánchez, and Raúl Antonino Feijóo. Multi-scale modelling of arterial tissue: Linking networks of fibres to continua. *Computer Methods in Applied Mechanics and Engineering*, 341:740–787, 2018.

[31] Andrey K Sarychev and Vladimir M Shalaev. Electromagnetic field fluctuations and optical nonlinearities in metal-dielectric composites. *Physics Reports*, 335(6):275–371, 2000.

[32] Abbas Sheikh Ansari, Ashwin K. Iyer, and Behrad Gholipour. Asymmetric transmission in nanophotonics. *Nanophotonics*, 12(14):2639–2667, 2023.

[33] A. Sihvola. *Electromagnetic mixing formulas and applications*. Number 47 in Electromagnetic Waves Series. Institute of Electrical Engineers, United Kingdom, 1999.

[34] M.G. Silveirinha. Metamaterial homogenization approach with application to the characterization of microstructured composites with negative parameters. *Physical Review B*, 75:115104, 2007.

[35] D.R. Smith, J.B. Pendry, and M.C.K. Wiltshire. Metamaterials and negative refractive index. *Science*, 305(5685):788–792, 2004.

[36] D.R. Smith, D.C. Vier, Th. Koschny, and C.M. Soukoulis. Electromagnetic parameter retrieval from inhomogeneous metamaterials. *Physical Review E - Statistical, Nonlinear, and Soft Matter Physics*, 71(3):036617, 2005.

[37] P.J. Sánchez, P.J. Blanco, A.E. Huespe, and R.A. Feijóo. Failure-oriented multi-scale variational formulation: Micro-structures with nucleation and evolution of softening bands. *Computer Methods in Applied Mechanics and Engineering*, 257:221–247, 2013.

[38] Igor Tsukerman and Vadim A. Markel. A non-asymptotic homogenization theory for periodic electromagnetic structures. *Proceedings of the Royal Society A: Mathematical, Physical and Engineering Sciences*, 470(2168):20140245, 2014.

[39] Ben-Xin Wang, Xuefeng Qin, Guiyuan Duan, Guofeng Yang, Wei-Qing Huang, and Zhiming Huang. Dielectric-based metamaterials for near-perfect light absorption. *Advanced Functional Materials*, page 2402068, 2024.

[40] Honggang Wang, Feifan Zheng, Yihan Xu, Michael G. Mauk, Xianbo Qiu, Zhen Tian, and Lulu Zhang. Recent progress in terahertz biosensors based on artificial electromagnetic subwavelength structure. *TrAC - Trends in Analytical Chemistry*, 158:116888, 2023.

[41] Pan Wang, Alexey V. Krasavin, Lufang Liu, Yunlu Jiang, Zhiyong Li, Xin Guo, Limin Tong, and Anatoly V. Zayats. Molecular plasmonics with metamaterials. *Chemical Reviews*, 122(19):15031–15081, 2022.

[42] Zhongyang Wang, Kai Sun, Peitao Xie, Yao Liu, Qilin Gu, and Runhua Fan. Permittivity transition from positive to negative in acrylic polyurethane-aluminum composites. *Composites Science and Technology*, 188:107969, 2020.

[43] Claire M. Watts, Xianliang Liu, and Willie J. Padilla. Metamaterial electromagnetic wave absorbers. *Advanced Materials*, 24(23):OP98–OP120, 2012.

[44] Niklas Wellander and Gerhard Kristensson. Homogenization of the maxwell equations at fixed frequency. *SIAM Journal on Applied Mathematics*, 64(1):170–195, 2003.

[45] Y. Wu, J. Li, Z.Q. Zhang, and C.T. Chan. Effective medium theory for magnetodielectric composites: Beyond the long-wavelength limit. *Physical Review B*, 74:085111, 2006.

(P.J. Blanco) Laboratório Nacional de Computação Científica, Coordenação de Métodos Matemáticos e Computacionais, Av. Getúlio Vargas 333, 25651-075 Petrópolis - RJ, Brasil
Email address: pjblanco@lncc.br

(F.A. Pinheiro) Instituto de Física, Universidade Federal do Rio de Janeiro, Caixa Postal 68528, Rio de Janeiro, Rio de Janeiro 21941-972, Brazil
Email address: fpinheiro@if.ufrj.br

(A.A. Novotny) Laboratório Nacional de Computação Científica, Coordenação de Métodos Matemáticos e Computacionais, Av. Getúlio Vargas 333, 25651-075 Petrópolis - RJ, Brasil
Email address: novotny@lncc.br